

Journal Pre-proof

Long-term systemic administration of kynurenic acid brain region specifically elevates the abundance of functional CB₁ receptors in rats

Ferenc Zádor, Gábor Nagy-Grócz, Szabolcs Dvorácskó, Zsuzsanna Bohár, Edina Katalin Cseh, Dénes Zádori, Árpád Párdutz, Edina Szűcs, Csaba Tömböly, Anna Borsodi, Sándor Benyhe, László Vécsei

PII: S0197-0186(20)30143-1

DOI: <https://doi.org/10.1016/j.neuint.2020.104752>

Reference: NCI 104752

To appear in: *Neurochemistry International*

Received Date: 10 April 2020

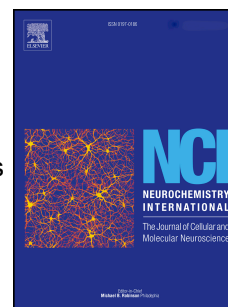
Revised Date: 7 May 2020

Accepted Date: 8 May 2020

Please cite this article as: Zádor, F., Nagy-Grócz, G., Dvorácskó, S., Bohár, Z., Cseh, E.K., Zádori, D., Párdutz, Á., Szűcs, E., Tömböly, C., Borsodi, A., Benyhe, S., Vécsei, L., Long-term systemic administration of kynurenic acid brain region specifically elevates the abundance of functional CB₁ receptors in rats, *Neurochemistry International*, <https://doi.org/10.1016/j.neuint.2020.104752>.

This is a PDF file of an article that has undergone enhancements after acceptance, such as the addition of a cover page and metadata, and formatting for readability, but it is not yet the definitive version of record. This version will undergo additional copyediting, typesetting and review before it is published in its final form, but we are providing this version to give early visibility of the article. Please note that, during the production process, errors may be discovered which could affect the content, and all legal disclaimers that apply to the journal pertain.

© 2020 The Author(s). Published by Elsevier Ltd.



Author Statement

Ferenc Zádor: Conceptualization, Methodology, Validation, Formal Analysis, Investigation, Writing-Original Draft, Visualization, Supervision, Project administration. **Gábor Nagy-Grócz:** Conceptualization, Methodology, Validation, Investigation, Resources, Writing - Review & Editing, Project administration. **Szabolcs Dvorácskó:** Conceptualization, Methodology, Validation, Investigation, Resources, Writing - Review & Editing. **Zsuzsanna Bohár:** Methodology, Validation, Investigation, Resources, Writing - Review & Editing. **Edina Katalin Cseh:** Methodology, Validation, Formal Analysis, Investigation, Writing - Review & Editing. **Dénes Zádori:** Writing - Review & Editing, Supervision, Funding acquisition. **Árpád Párdutz:** Conceptualization, Writing - Review & Editing. **Edina Szűcs:** Resources, Writing - Review & Editing. **Csaba Tömböly:** Writing - Review & Editing, Supervision, Funding acquisition. **Anna Borsodi:** Conceptualization, Writing - Review & Editing. **Sándor Benyhe:** Writing - Review & Editing, Supervision, Funding acquisition. **László Vécsei:** Writing - Review & Editing, Supervision, Funding acquisition.

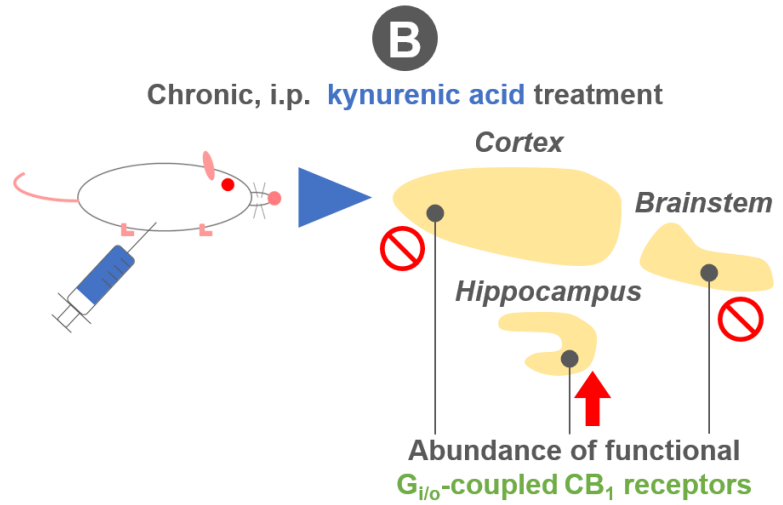
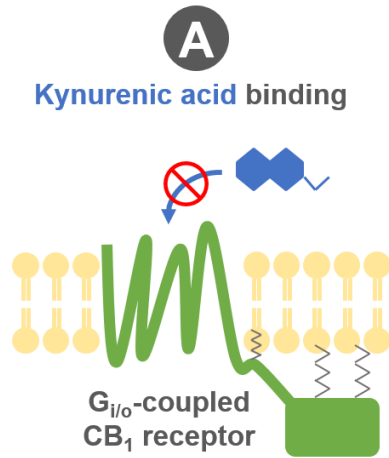


Table 1. CB₁R affinity (K_i) and CB₁R-mediated G-protein efficacy (E_{max}) and ligand potency (EC_{50}) values of KYNA and the CB₁R selective ACEA alone and in combination with KYNA. K_i values of the non-selective CBR ligand WIN55,212-2 and the CB₂R selective CB65 ligand is also indicated for control and for comparison. The indicated parameters were calculated from the concentration-effect curves presented in Figure 2A (K_i) and B (E_{max} , EC_{50}) and were statistically analyzed as discussed in section **ERROR! REFERENCE SOURCE NOT FOUND.**

<i>Compounds</i>	CB₁R affinity ([³ H]WIN55,212-2 binding)		G-protein activity ([³⁵ S]GTP γ S binding)		
	$K_i \pm S.E.M. (nM)$	n	$E_{max} \pm S.E.M. (\%)$	$EC_{50} \pm S.E.M. (nM)$	n
KYNA	not relevant ¹	4	100.9 \pm 1.22	not relevant ¹	3
ACEA	202.9 \pm 55.28	4	170.2 \pm 6.55	137.72 \pm 53.22	3
ACEA + 10 μM KYNA	214.92 \pm 40.26	4	164.4 \pm 6.43	129.12 \pm 52.55	3
WIN55,212-2	3.74 \pm 0.89	4		N.D.	
CB65	>1000	4		N.D.	

¹: Total specific binding (100%) was not altered significantly (one-sample t test with 100 % theoretical value), thus K_i value calculation is not relevant

²: [³H]WIN55,212-2 binding was only reduced to 62 %.

N.D.: not determined.

Table 2. KYNA concentration levels in plasma and CSF following systemic KYNA chronic treatment (i.p., 9 days, 128 mg/kg/day). Experiments were analyzed and performed as described in section **ERROR! REFERENCE SOURCE NOT FOUND.** and **ERROR! REFERENCE SOURCE NOT FOUND.**, respectively.

Plasma		CSF	
<i>Concentration \pm S.E.M. (nM)</i>		<i>Concentration \pm S.E.M. (nM)</i>	
<i>Vehicle</i>	<i>KYNA</i>	<i>Vehicle</i>	<i>KYNA</i>
63.95 \pm 7.95 (n=5)	307.58 \pm 60.44** (n=5)	3.32 \pm 1.32 ^{###} (n=5)	10.69 \pm 2.04*/ ^{##} (n=4)

*: indicates the significant difference compared to vehicle (unpaired t test, two-tailed P value).

#: indicates the significant difference compared to their corresponding group measured in the plasma (unpaired t test, two-tailed P value).

Table 3. The effect of long-term systemic KYNA treatment (i.p., 9 days, 128 mg/kg/day) compared to vehicle on CB₁R-coupled G-protein activity in rat brain membranes described by the indicated parameters obtained from [³⁵S]GTPγS binding assays. CB₁R was stimulated by the highly CB₁R selective agonist ACEA and inverse agonist rimonabant. The table highlights the non-specific binding (NS), basal activity (*Basal*) and maximum efficacy (*E_{max}*) levels of CB₁R-coupled G-protein activity upon receptor stimulation given in specifically bound [³⁵S]GTPγS of protein content. *E_{max}* levels and ligand potency (*EC₅₀*) values were also calculated when data were normalized to basal activity levels (100 %) to see the overall performance of the ligands. Data were obtained from concentration-effect curves shown in Fig. 3 and statistically analyzed based on section **ERROR! REFERENCE SOURCE NOT FOUND.**

Compounds	Treatment (n)	Normalized to protein content			Normalized to basal activity	
		NS ± S.E.M. (fmol/mg)	Basal ± S.E.M. (fmol/mg)	<i>E_{max}</i> ± S.E.M. (fmol/mg)	<i>E_{max}</i> ± S.E.M. (%)	<i>EC₅₀</i> ± S.E.M. (nM)
ACEA	Vehicle (5)	19.89 ± 1.89	40.43 ± 8.52	61.76 ± 14.57	153.3 ± 6.99	1059.25 ± 626.93
	KYNA (8)	23.77 ± 1.39	85.18 ± 13.12*	124 ± 15.95*	152.6 ± 5.6	1713.96 ± 902.28
Rimonabant	Vehicle (7)	20.6 ± 1.13	50.56 ± 2.85	12.1 ± 3.78	14.8 ± 6.86	1870.68 ± 601.76
	KYNA (7)	22.92 ± 1.55	81.73 ± 2.74***	26.6 ± 4.41*	27.91 ± 4.74	2004.47 ± 478.91

*: significant difference compared to vehicle treated (unpaired t test, two-tailed P value; *: P < 0.05; ***: P < 0.001

NS: non-specific binding

Table 4. The effect of long-term systemic KYNA treatment (i.p., 9 days, 128 mg/kg/day) on CB₁R maximum binding capacity (B_{max}) and binding affinity (dissociation constant; K_d) in saturation binding assays using [³H]WIN55,212-2 radioligand to detect CB₁Rs in rat brain membranes. Data were obtained and analyzed from concentration-effect curves presented in Fig. 4 as described in section **ERROR! REFERENCE SOURCE NOT FOUND.**

<i>Treatment (n)</i>	[³H]WIN55,212-2 saturation binding	
	<i>B_{max} ± S.E.M. (fmol/mg)</i>	<i>K_d ± S.E.M. (nM)</i>
Vehicle (4)	1339.25 ± 54.79	9.17 ± 1.04
KYNA (4)	1879.09 ± 54.44***	11.69 ± 0.91

*: significant difference compared to vehicle treated (unpaired t test, two-tailed P value; ***: P < 0.001)

Table 5. The effect of long-term systemic KYNA treatment (i.p., 9 days, 128 mg/kg/day) compared to vehicle on CB₁R-coupled G-protein activity in rat cortex, hippocampus and brainstem described by the indicated parameters obtained from [³⁵S]GTPγS binding assays. CB₁R was stimulated by the highly CB₁R selective agonist ACEA in increasing concentrations. The table highlights the non-specific binding (*NS*), basal activity (*Basal*) and maximum efficacy (*E_{max}*) levels of CB₁R-coupled G-protein activity upon receptor stimulation given in specifically bound [³⁵S]GTPγS of protein content. *E_{max}* levels and ligand potency (*EC₅₀*) values were also calculated when data were normalized to basal activity levels (100 %) to see the overall performance of the ligand. Data were obtained from concentration-effect curves shown in Fig. 5 and statistically analyzed based on section **ERROR!** **REFERENCE SOURCE NOT FOUND..**

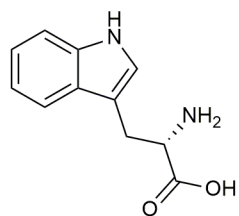
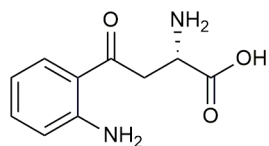
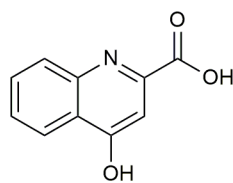
Brain region	Treatment (n)	Normalized to protein content			Normalized to basal activity	
		<i>NS</i> ± <i>S.E.M.</i> (fmol/mg)	<i>Basal</i> ± <i>S.E.M.</i> (fmol/mg)	<i>E_{max}</i> ± <i>S.E.M.</i> (fmol/mg)	<i>E_{max}</i> ± <i>S.E.M.</i> (%)	<i>EC₅₀</i> ± <i>S.E.M.</i> (nM)
Cortex	Vehicle (3)	5.53 ± 0.18	60.09 ± 6.28	96.03 ± 12.69	159.8 ± 5.92	189.23 ± 74.34
	KYNA (3)	5.47 ± 0.03	61.28 ± 3.39	97.96 ± 7.19	160.2 ± 6.4	243.22 ± 97.66
Hippocampus	Vehicle (6)	6.49 ± 0.44	84.7 ± 6.45	161.7 ± 8.71	193.1 ± 4.56	130.32 ± 24.69
	KYNA (5)	7.42 ± 0.25	119.5 ± 4.46**	217.3 ± 11.93**	186.7 ± 6.28	161.81 ± 38.66
Brainstem	Vehicle (6)	9.91 ± 3.02	26.34 ± 2.84	36.39 ± 4.17	129.8 ± 1.92	91.41 ± 20.23
	KYNA (4)	9.91 ± 4.49	26.52 ± 6.73	33.18 ± 9.55	130.3 ± 1.92	96.16 ± 22.88

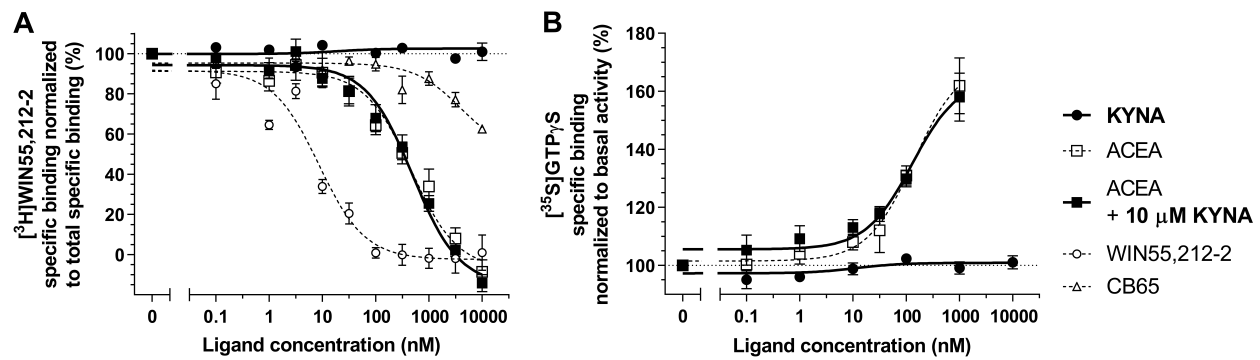
*: significant difference compared to vehicle treated (unpaired t test, two-tailed P value; **: P < 0.01)

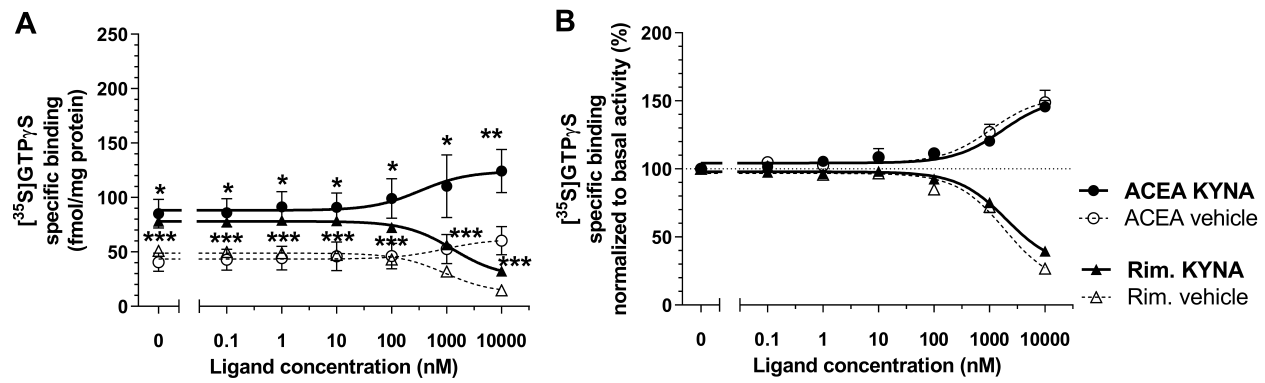
Table 6. The effect of long-term systemic KYNA treatment (i.p., 9 days, 128 mg/kg/day) in rat hippocampus on CB₁R maximum binding capacity (B_{max}) and binding affinity (dissociation constant; K_d) in saturation binding assays using [³H]WIN55,212-2 radioligand to detect CB₁Rs. Data were obtained and analyzed from concentration-effect curves presented in Fig. 6 as described in section **ERROR! REFERENCE SOURCE NOT FOUND.**

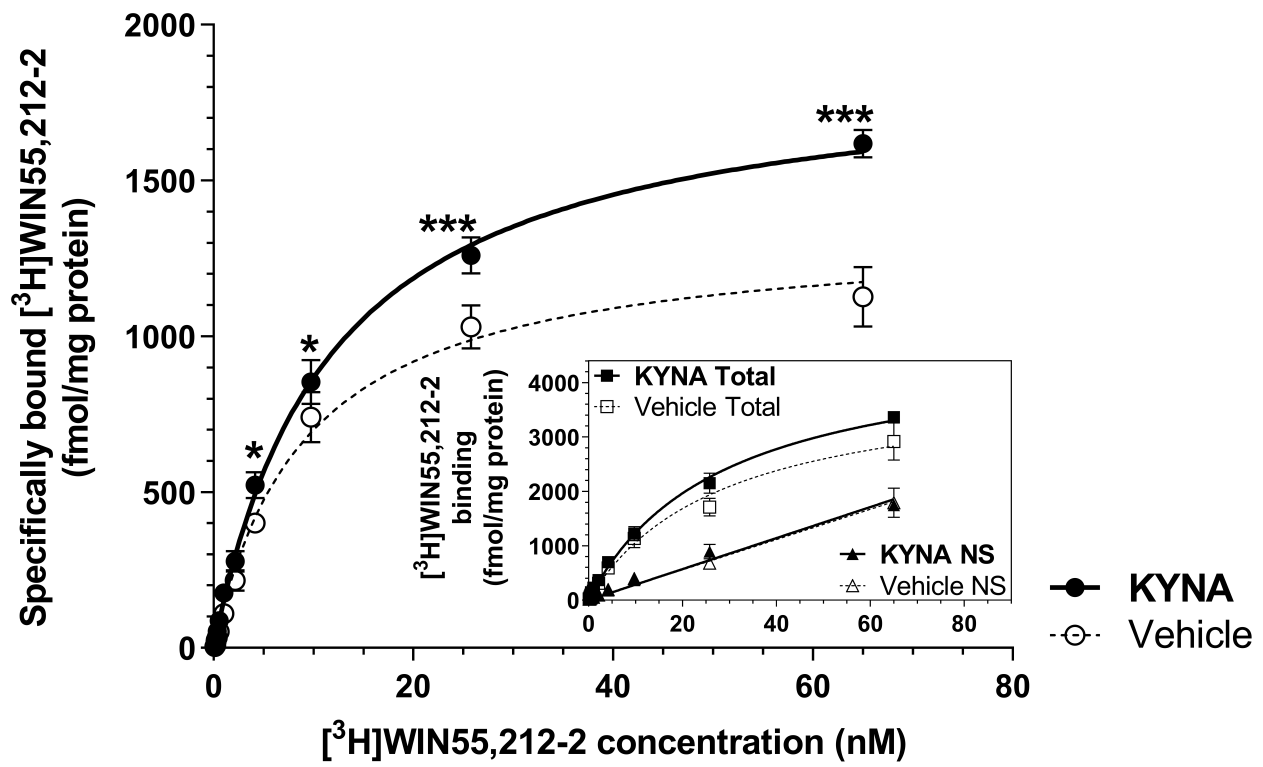
<i>Treatment (n)</i>	[³H]WIN55,212-2 specific binding	
	$B_{max} \pm S.E.M. (fmol/mg)$	$K_d \pm S.E.M. (nM)$
Vehicle (4)	1069.16 \pm 96.83	13.39 \pm 2.98
KYNA (4)	1403.23 \pm 75.36*	16.74 \pm 2.07

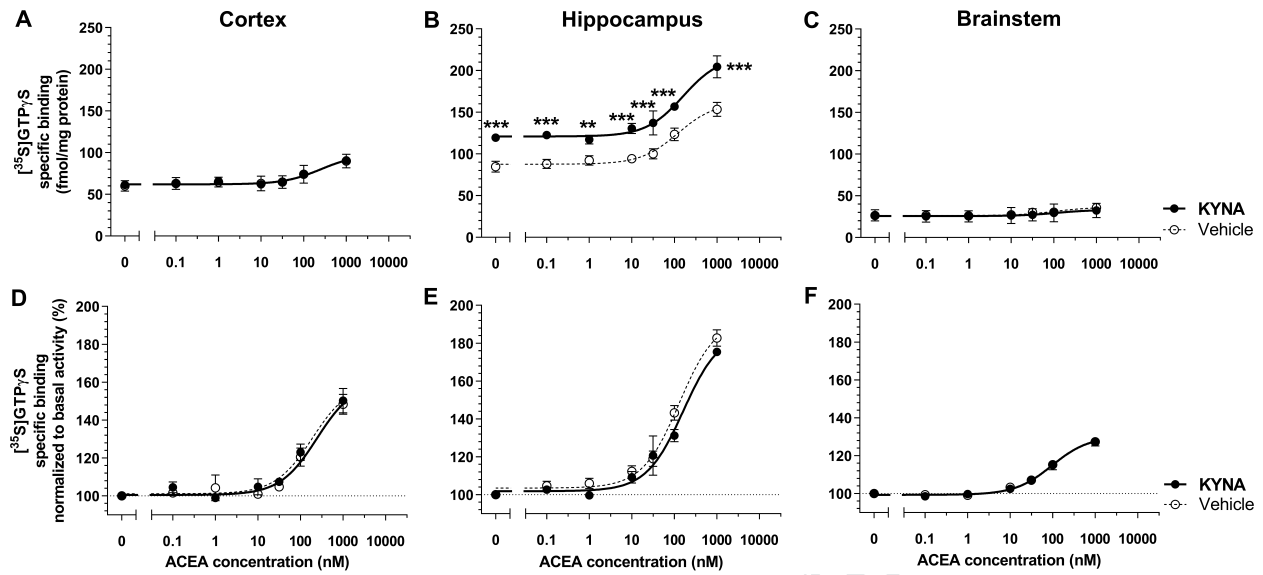
*: significant difference compared to vehicle treated (unpaired t test, two-tailed P value)

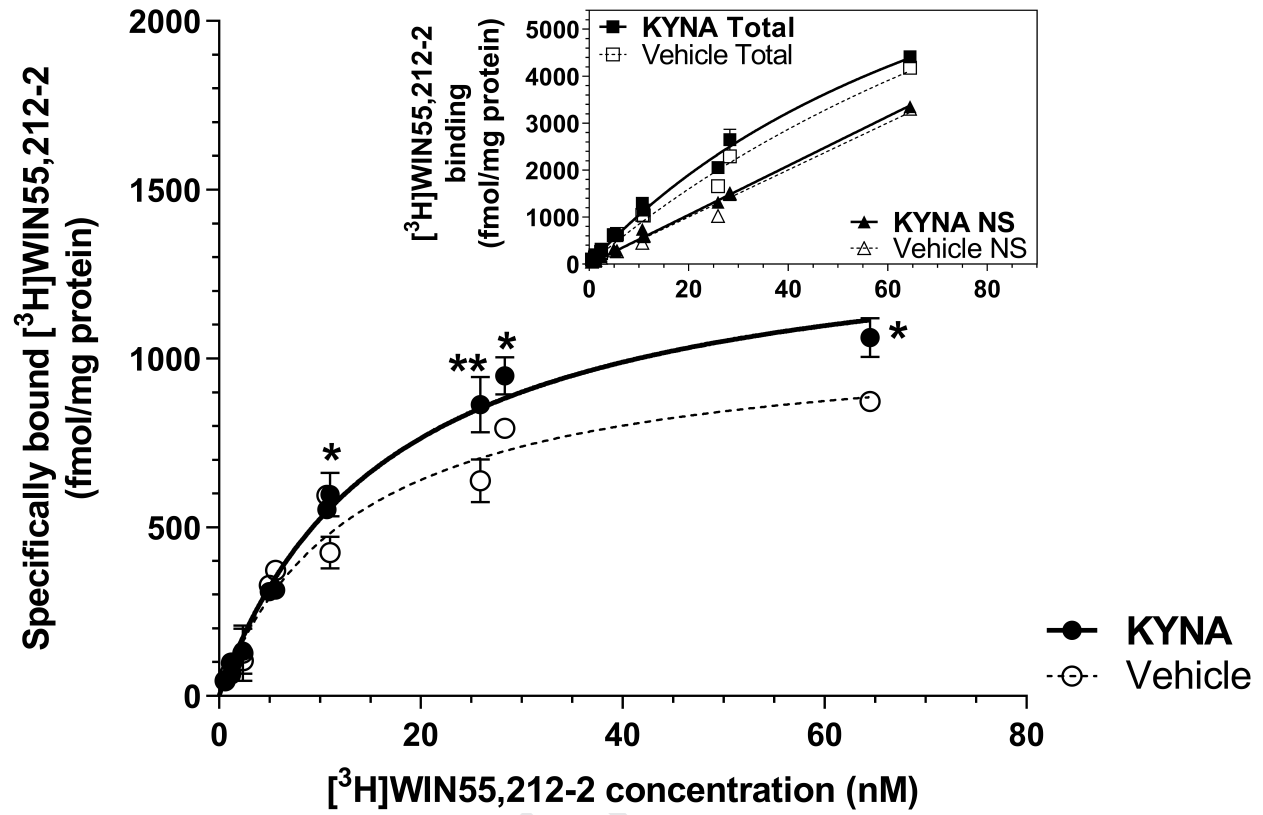
**L-tryptophan****L-kynurenine****kynurenic acid**











HIGHLIGHTS:

- Kynurenic acid (KYNA) does not interact directly with CB₁Rs.
- Chronic, systemic KYNA treatment elevates KYNA CSF and plasma levels.
- The same treatment increases the amount of functional CB₁Rs in the whole brain.
- The treatment does not affect the binding and the activity of the receptor.
- Such results also apply to the hippocampus, but not to the cortex or brainstem.

Long-term systemic administration of kynurenic acid brain region specifically elevates the abundance of functional CB₁ receptors in rats

Ferenc Zádor^{a,1,*;†}, Gábor Nagy-Grócz^{b,c,*}, Szabolcs Dvorácskó^{a,d}, Zsuzsanna Bohár^{c,e}, Edina Katalin Cseh^c, Dénes Zádori^c, Árpád Párdutz^c, Edina Szűcs^{a,f}, Csaba Tömböly^a, Anna Borsodi^a, Sándor Benyhe^a, László Vécsei^{c,e}

^a: Institute of Biochemistry, Biological Research Centre, Szeged, Temesvári krt. 62., H-6726, Hungary

^b: Faculty of Health Sciences and Social Studies, University of Szeged, Szeged, Temesvári krt. 31., H-6726, Hungary

^c: Department of Neurology, Interdisciplinary Excellence Center, Faculty of Medicine, Albert Szent-Györgyi Clinical Center, University of Szeged, Szeged, Semmelweis u. 6., H-6725, Hungary

^d: Department of Medical Chemistry University of Szeged, Szeged, Dóm tér 8., H-6720, Hungary

^e: MTA-SZTE Neuroscience Research Group, University of Szeged, H-6725 Szeged, Hungary

^f: Doctoral School of Theoretical Medicine, Faculty of Medicine, University of Szeged, Dóm tér 10., H-6720 Szeged, Hungary

¹: Present address: Department of Pharmacology and Pharmacotherapy, Faculty of Medicine, Semmelweis University, Nagyvárad tér 4, P.O. Box 370, H-1445 Budapest, Hungary

*: These authors contributed equally to the work

[†]: Corresponding author:
Email address: zador.ferenc@gmail.com
Phone: +36-1-210-4405

This work is dedicated to the late Prof. Maria Wollemann

ABSTRACT

Kynurenic acid (KYNA) is one of the most significant metabolite of the kynurenine pathway both in terms of functional and potential therapeutic value. It is an *N*-methyl-D-aspartate (NMDA) receptor antagonist, but it can also activate the G-protein coupled receptor 35 (GPR35), which shares several structural and functional properties with cannabinoid receptors. Previously our group demonstrated that systemic chronic KYNA treatment altered opioid receptor G-protein activity. Opioid receptors also overlap in many features with cannabinoid receptors. Thus, our aim was to examine the direct *in vitro* and systemic, chronic *in vivo* effect of KYNA on type 1 cannabinoid receptor (CB₁R) binding and G-protein activity.

Based on competition and [³⁵S]GTPγS G-protein binding assays in rat brain, KYNA alone did not show significant binding towards the CB₁R, nor did it alter CB₁R ligand binding and agonist activity *in vitro*. When rats were chronically treated with KYNA (single daily, i.p., 128 mg/kg for 9 days), the KYNA plasma and cerebrospinal fluid levels significantly increased compared to vehicle treated group. Furthermore, in G-protein binding assays, in the whole brain the amount of G-proteins in basal and in maximum activity coupled to the CB₁R also increased due to the treatment. At the same time, the overall stimulatory properties of the receptor remained unaltered in vehicle and KYNA treated samples. Similar observations were made in rat hippocampus, but not in the cortex and brainstem. In saturation binding assays the density of CB₁Rs in rat whole brain and hippocampus were also significantly enhanced after the same treatment, without significantly affecting ligand binding affinity.

Thus, KYNA indirectly and brain region specifically increases the abundance of functional CB₁Rs, without modifying the overall binding and activity of the receptor. Supposedly, this can be a compensatory mechanism on the part of the endocannabinoid system induced by the long-term KYNA exposure.

Keywords: type 1 cannabinoid receptor; kynurenic acid; G-protein; [³⁵S]GTPγS binding; radioligand binding; hippocampus

ABBREVIATIONS:

[³⁵S]GTP γ S, guanosine-5'-O-(3-[³⁵S]thio)triphosphate

ACEA, arachidonyl-2'-chloroethylamide

BBB, blood-brain-barrier

B_{max}, maximum binding capacity

CB₁R, type 1 cannabinoid receptor

CNS, central nervous system

CSF, cerebrospinal fluid

EC₅₀, 50 % effective concentration

ECS, endocannabinoid system

EGTA, ethyleneglycol-tetraacetate

E_{max}, maximum efficacy

GDP, guanosine 5'-diphosphate

GPCR, G-protein coupled receptor

GPR35, G-protein coupled receptor 35

GTP, guanosine 5'-triphosphate

GTP γ S, Guanosine-5'-O-[γ -thio] triphosphate

HPLC, high-performance liquid chromatography

K_d, dissociation constant

K_i, inhibitory constant

KP, kynurenine pathway

KYNA, kynurenic acid

L-KYN, L-kynurenine

NMDAR, N-methyl-D-aspartate receptor

Tris-HCl, tris-(hydroxymethyl)-aminomethane hydrochloride

1 INTRODUCTION

The endocannabinoid system (ECS) is comprised of the lipid-like endogenous cannabinoids (endocannabinoids), their synthesizing and metabolizing enzymes and the G-protein coupled cannabinoid receptors (CB₁R and CB₂R), which mediate their effects (Rodríguez de Fonseca et al., 2005). The ECS is a major neuromodulator system maintaining the tones of several physiological processes (Rodríguez de Fonseca et al., 2005). The CB₁R is the most abundant G-protein coupled receptor (GPCR) in the central nervous system (CNS), its density is comparable to that of the glutamate, γ -aminobutyric acid (GABA) and dopamine receptors (Herkenham et al., 1990; Matsuda et al., 1990; Piomelli, 2003). It can also be found in the periphery such as in adipose tissues, cardiovascular and gastrointestinal system (Maccarrone et al., 2015; Pagotto et al., 2006). CB₁Rs belong to the class A GPCR superfamily and they mostly couple to the G_{i/o} type inhibitory G-protein. Thus, their activation inhibits cyclic adenosine monophosphate (cAMP) production and L-type Ca²⁺ channel activity as well as stimulates K⁺ channels (Howlett et al., 2002). Overall these signal transductions will eventually inhibit the release of several types of neurotransmitters, such as acetylcholine, GABA, noradrenaline or dopamine (Howlett et al., 2002). These induced changes allow the CB₁Rs to be involved for instance in the regulation of mood, energy balance and endocrine functions (Maccarrone et al., 2015; Pagotto et al., 2006; Pertwee, 2009).

The kynurenine pathway (KP) is the main route of tryptophan (Fig. 1) catabolism and kynurenic acid (KYNA; Fig. 1) - a side product of L-kynurenine (L-KYN; Fig. 1) - is recognized as a potent neuroprotective molecule in several experimental models (Carrillo-Mora et al., 2010; Chen et al., 2011; Knyihar-Csillik et al., 2008; Lee et al., 2008; Oláh et al., 2013; Silva-Adaya et al., 2011). It has been also well documented that the level of KYNA concentration in the brain is relevant in multiple neurological diseases (Bortz et al., 2017; Vécsei et al., 2013). KYNA is an endogenous ligand for multiple receptors, such as the *N*-methyl-D-aspartate receptor (NMDAR) and other ionotropic glutamate receptors (Birch et al., 1988; Perkins and Stone, 1985), and the G-protein coupled receptor 35 (GPR35) (Wang et al., 2006).

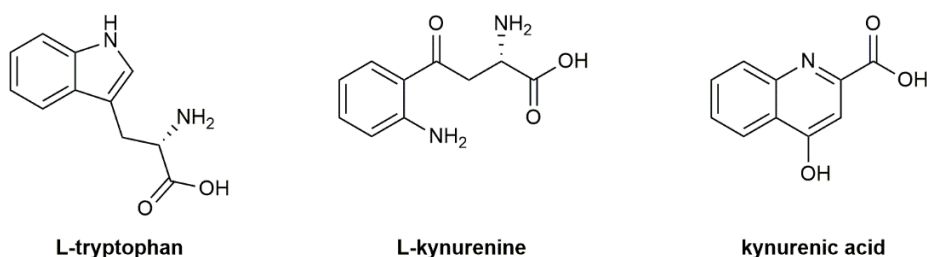


Figure 1. Chemical structure of L-tryptophan, L-kynurenine and kynurenic acid.

Previously we demonstrated that chronic KYNA treatment significantly altered opioid receptor G-protein activity depending on receptor type and brain region, without binding directly to the opioid receptors (Zádor et al., 2014b). This effect also appeared after acute treatments, and the involvement of the NMDAR was also demonstrated (Samavati et al., 2017). In addition, opioid peptides incorporating L-KYN and KYNA have been synthesized and characterized recently, which compounds displayed significant opioid receptor binding, agonist activity and antinociceptive effect (Szűcs et al., 2020). Opioid receptors share similar structural and functional properties with cannabinoid receptors (Viganò et al., 2005), moreover their heterodimerization can be exploited with opioid-cannabinoid bivalent compounds for the development of safer analgesics (Dvoráček et al., 2019; Fernández-Fernández et al., 2014; Le Naour et al., 2013; Mollica et al., 2017). More importantly, cannabinoid receptors also resemble to the KYNA activated GPR35 in G-protein signaling, structure, distribution and function (Shore and Reggio, 2015; Wang et al., 2006). Furthermore, exogenous cannabinoids are known to alter the activity of certain enzymes of the KP in a cannabinoid receptor-dependent manner in peripheral blood mononuclear cells (Jenny et al., 2009). Also, acute tetrahydrocannabinol (THC) treatment has been shown to reduce extracellular levels of KYNA through the CB₁R in brain reward processing areas (Secci et al., 2018). Thus, a potential cross-talk might be present between the members of KP (enzymes, metabolites) and the ECS. This is supported by overlapping functions in certain mechanisms such as dopamine, glutamate or GABA neurotransmission regulation (Beggiato et al., 2014; Fernández-Ruiz et al., 2010; Javitt et al., 2011; Stone et al., 2007) or immune regulation (Maccarrone et al., 2015; Mándi and Vécsei, 2012). Finally, Beggiato and co-workers recently demonstrated that long-term prenatal THC exposure significantly increases KYNA levels in the prefrontal cortex of adult rats (Beggiato et al., 2020). In the same study they also showed that after a low dose, acute and systemic KYN treatment in adulthood, the increase of

KYNA levels in the prefrontal cortex was more pronounced in prenatally THC-exposed rats (Beggiato et al., 2020).

Considering the above mentioned data we designed a set of experiments to investigate for the first time the direct binding/interaction of KYNA to the CB₁R in receptor binding and G-protein activity measurements. The CB₁R was chosen because it is the most widely studied cannabinoid receptor of the ECS. Additionally, the effect of a long-term KYNA treatment was examined on G-protein activity and CB₁R binding, using the same treatment protocol as applied for opioid receptors previously (Zádor et al., 2014b). In these experiments, initially whole brain membranes were investigated after the treatment. The cortex, the hippocampus and the brainstem was further analyzed the same way, since these regions are rich in CB₁Rs (Herkenham et al., 1990) and/or mediate important cellular functions.

2 MATERIALS AND METHODS

2.1 Chemicals

Tris-HCl, ethylene glycol-bis(β -aminoethyl ether)-N,N,N',N'-tetraacetic acid (EGTA), NaCl, $\text{MgCl}_2 \times 6\text{H}_2\text{O}$, guanosine diphosphate (GDP), the guanosine triphosphate (GTP) analogue GTP γ S and kynurenic acid (KYNA) were purchased from Sigma-Aldrich (St. Louis, MO, USA). Fatty acid free bovine serum albumin (BSA) was purchased from Serva (Heidelberg, Germany). The CB₁R specific agonist and inverse agonist arachidonyl-2'-chloroethylamide (ACEA) and rimonabant, respectively and the non-selective cannabinoid receptor agonist WIN55,212-2 were purchased from Tocris Bioscience (Budapest, Hungary). The radiolabeled GTP analogue, [³⁵S]GTP γ S (specific activity: 37 TBq/mmol; 1000 Ci/mmol) was obtained from Hartmann Analytic (Braunschweig, Germany). The tritiated WIN55,212-2 ([³H]WIN55,212-2) was radiolabeled in the Laboratory of Chemical Biology (Biological Research Centre, Szeged, Hungary; specific activity: 485 GBq/mmol) (Szűcs et al., 2016). The UltimaGoldTM MV aqueous scintillation cocktail was purchased from PerkinElmer (Per-form kft, Budapest, Hungary). KYNA for receptor assays was dissolved in highly pure distilled water, while cannabinoid compounds were dissolved in dimethyl sulfoxide. All compounds were stored in 1 mM stock solution at -20 °C. All chemicals and reagents used for the high-performance liquid chromatography (HPLC) measurements were of analytical or HPLC grade, and they were acquired from Sigma-Aldrich (St. Louis, MO, USA). The internal standard used for the fluorescent detector, was synthesized at the Department of Pharmaceutical Chemistry, University of Szeged, as detailed elsewhere (Cseh et al., 2019).

2.2 Animals, treatments and sample extraction

Throughout the study, 47 male Sprague-Dawley rats were used; the animals were 8-10 weeks of age, with an average body weight of 250-350 g. For HPLC measurements 6, for whole brain and brain region specific receptor binding assays 8 and 7 animals per group were used, respectively. In KYNA affinity and G-protein activity measurements overall 5 animals were sacrificed. The animals were bred and maintained under standard laboratory conditions on a 12-h dark 12-h light cycle at 22-24 °C and ~55% relative humidity with free access to water and food pellets. All experimental procedures were carried out in accordance with the European Communities Council Directive (2010/63/EU), and the Hungarian Act for the Protection of

Animals in Research (XXVIII.tv. 32.§). We did the best effort to minimize the number of animals and their suffering.

KYNA was dissolved in saline and the pH of the solutions was adjusted to 7.4 with 1 N NaOH. Rats were divided into two groups, KYNA and vehicle treated. KYNA was administered intraperitoneal (i.p.) in a dose of 128 mg/kg/day in a volume of 1 ml to each animal. The animals received the injections once a day in the morning, at the same time for 9 consecutive days based on our previous study (Zádor et al., 2014b). The control group received vehicle, which was 0.9 % saline. The treatments were well tolerated by the animals.

Four hours after the last injection, on the 9th day, rats were deeply anesthetized with chloral-hydrate (Sigma-Aldrich, Budapest, Hungary). Prior to perfusion, the cerebrospinal fluid (CSF) was taken quickly from the suboccipital cistern of rats with 23G needle to Eppendorf tubes (rats were placed to the stereotaxic setup in order to fix their head). Venous blood was collected from the left of the heart chamber to a tube containing EDTA as anticoagulant. Transcardial perfusion was performed with PBS (100 ml, 0.1 M, pH 7.4). The perfused brains were removed rapidly and in case of vehicle and KYNA treated samples the cerebellum was dissected, and the remaining brain area was stored or the cortex, hippocampus and brainstem were excised. For characterizing CB₁R binding and activity *in vitro* in the presence of KYNA, untreated perfused whole brain samples were used. Samples were stored at -80 °C until preparation for the *in vitro* experiments.

2.3 Receptor binding assays

2.3.1 Membrane preparation

The tissue samples were handled for membrane preparation according to Benyhe and co-workers (Benyhe et al., 1997). The membrane homogenates were used both for [³⁵S]GTPγS binding assays and for saturation binding studies according to Zádor and co-workers (Zádor et al., 2014a). In brief, the samples from the same treatment group and brain region were pooled together and were homogenized, centrifuged in ice-cold TEM buffer (50 mM Tris-HCl, 1 mM EGTA, 3 mM MgCl₂, 100 mM NaCl, pH 7.4) and then incubated at 37 °C for 30 min in a shaking water-bath. After incubation, the centrifugation was repeated and the final pellet was again suspended in TEM buffer (pH 7.4). From hippocampus samples membrane fractions were not prepared; they were only homogenized. This was to limit the number of sacrificed animals. Due

to the small size of the rat hippocampus, unnecessary number of animals would have been sacrificed for the assays to obtain membrane fractions with adequate protein content. Protein concentrations of the samples were measured by the Bradford method and samples were diluted to obtain the appropriate amount for the assay as described below. Samples were stored -80 °C for further use.

2.3.2 Radioligand competition binding assays

In competition binding assays the specific binding of a receptor selective radioligand is measured in the presence of increasing concentrations of an unlabeled compound (Frey and Albin, 2001). The concentration dependent decrease of radioligand specific binding provides information of the binding affinity of the unlabeled compound by determining the concentration range of 50 % inhibition and the inhibitory constant (IC_{50} , K_i).

Whole brain membrane homogenates containing 0.5 mg/ml of protein were incubated in the presence of 50 mM Tris-HCl, 2.5 mM EGTA, 5 mM $MgCl_2$ and 0.5 mg/ml fatty acid-free BSA (pH 7.4) together with increasing concentrations (0.1 nM-10 μ M) of KYNA, ACEA (in the absence or presence of 10 μ M KYNA), WIN55,212-2 and CB65, with ~ 1-3 nM concentrations of [3H]WIN55,212-2. The non-specific and total binding was determined in the presence of 10 μ M unlabeled WIN55,212-2 and in the absence of unlabeled compounds, respectively. Following a 60 min incubation at 30 °C, the reaction was terminated by rapid filtration under vacuum (Brandel M24R Cell Harvester), and washed three times with ice-cold 50 mM Tris-HCl, 2.5 mM EGTA, 5 mM $MgCl_2$ and 0.5 mg/ml fatty acid-free BSA (pH 7.4) through Whatman GF/B glass fiber filters (GE Healthcare Life Sciences through Izinta Kft., Budapest, Hungary). The radioactivity of the filters was counted in UltimaGoldTM MV aqueous scintillation cocktail with Packard Tricarb 2300TR liquid scintillation analyzer.

2.3.3 Functional [^{35}S]GTP γ S binding assays

In [^{35}S]GTP γ S binding experiments the GDP→GTP exchange of the G_α protein is monitored in the presence of a given compound in increasing concentrations to measure ligand potency (EC_{50}) and the maximal effect (efficacy; E_{max}) of receptor G-protein (Strange, 2010). The nucleotide exchange is monitored by a radioactive, non-hydrolysable GTP analog, [^{35}S]GTP γ S.

The functional [^{35}S]GTP γ S binding experiments were performed as previously described (Selley et al., 1997; Traynor and Nahorski, 1995), with modifications. Briefly, the brain samples containing 30 $\mu\text{g}/\text{ml}$ protein were incubated at 30 °C for 60 min in Tris-EGTA buffer (pH 7.4) composed of 50 mM Tris-HCl, 1 mM EGTA, 3 mM MgCl_2 , 100 mM NaCl contained 0.05 nM [^{35}S]GTP γ S and increasing concentrations (0.1 nM-10 μM) of KYNA, ACEA (in the presence or absence of 10 μM KYNA) or rimonabant and excess GDP (30 μM) in a final volume of 1 ml. Such assay protocol has been shown to be optimized for monitoring $\text{G}_{i/o}$ -type G-proteins (DeLapp et al., 2004). Total binding was measured in the absence of ligands, while non-specific binding was determined in the presence of 10 μM unlabeled GTP γ S. The bound and unbound [^{35}S]GTP γ S were separated by rapid filtration under vacuum (Brandel M24R Cell Harvester) through Whatmann GF/B glass fibers and washed three times with ice-cold 50 mM Tris-HCl (pH 7.4). The radioactivity of the filters was measured as described in section 2.3.2.

2.3.4 Saturation binding assays

With saturation binding experiments we can determine the maximum binding capacity of a receptor (B_{max}), which also indicates the density of the given receptor in the examined tissue sample (Frey and Albin, 2001). This is done by saturating the receptor with a radioligand specific to that receptor protein applying it in increasing concentrations. Additionally, the affinity of the radioligand can also be determined with the dissociation constant (K_d).

In saturation binding assays membrane preparations containing 0.4 mg/ml of protein were incubated in the presence of 50 mM Tris-HCl, 2.5 mM EGTA, 5 mM MgCl_2 and 0.5 mg/ml fatty acid-free BSA (pH 7.4), together with increasing concentrations of [^3H]WIN55,212-2 (0.13–65 nM) in the absence (total binding) or presence (non-specific binding) of 10 μM WIN55,212-2. Following incubation (60 min, 30 °C), the bound and unbound [^3H]WIN55,212-2 were separated and the radioactivity of the samples were measured as described in section 2.3.2.

2.4 HPLC measurements

Validated HPLC methods were performed by an Agilent 1100 HPLC system (Santa Clara, CA, USA), coupled with UV detector (UVD) and fluorescence detector (FLD). The chromatographic separation, and the validation process was described elsewhere (Cseh et al., 2019). Briefly, the brain regions were homogenized in 0.5 M perchloric acid (PCA), at 1:5 w/v containing the internal standards (ISs) 3-nitro-L-tyrosine (3-NLT) and 4-hydroxyquinazoline-2-carboxylic acid (HCA) at a final concentration of 2 μ M and 100 nM, respectively. The precipitate was separated by centrifugation for 10 min at 12000 rpm at 4 °C. As for the plasma and CSF samples, both were deproteinized with 0.5 M PCA solution, 1:1 v/v and 5:6 v/v respectively, then the above-mentioned centrifugation process was applied. Afterwards, the chromatographic separations were performed on a reversed-phase C18 column (Kinetex, 150 \times 4.6mm I.D., 5 μ m particle size; Phenomenex Inc., Torrance, CA, USA) with a mobile phase composition of 200 mM zinc acetate, at final pH of 5.8 for brain tissue samples and 6.2 for plasma and CSF samples, with a final concentration of 5 % of acetonitrile in each case. Blinded HPLC measurements were conducted to eliminate experimental biases.

2.5 Data analysis

In receptor binding assays, the specific binding of the given radiolabeled compound ($[^3\text{H}]\text{WIN55,212-2}$, $[^{35}\text{S}]\text{GTP}\gamma\text{S}$) was calculated by subtracting the non-specific binding from the total binding. Data were normalized either to total specific binding or either to protein content presented in fmol/mg. Total specific binding was set 100 %, which represented the basal activity level of G-protein in the case of $[^{35}\text{S}]\text{GTP}\gamma\text{S}$ measurements. The means \pm S.E.M. (standard error of mean) of data sets were plotted in the function of the applied ligand concentration in logarithmic scale (except for saturation binding) and were fitted with GraphPad Prism 7.0 (GraphPad Prism Software Inc., San Diego, CA), by non-linear regression. For competition binding assays the ‘One-site competition’ equation was used to determine the IC_{50} value (unlabeled ligand affinity) and to calculate the inhibitory constant (K_i) value according to the Cheng-Prusoff equation (Cheng and Prusoff, 1973). Experimental data of $[^{35}\text{S}]\text{GTP}\gamma\text{S}$ binding assays were fitted with the ‘Sigmoid dose-response’ equation to obtain maximum efficacy (E_{max}) and ligand potency (EC_{50}) values. Saturation binding data were fitted with ‘One-site - specific binding’ equation to visualize maximum binding capacity (B_{max}) and dissociation constant (K_d)

values. Additionally, in these assays non-specific binding was also plotted with linear regression to compare slopes.

In the HPLC analysis, the relative peak area responses (analyte/internal standard) were plotted against the corresponding concentration, and the linear regression computations were carried out by the least square method with the R software 3.5.3 (R Core Team, 2014).

For two data sets unpaired t test with two-tailed P value, for more than two data sets two-way ANOVA with uncorrected Fisher's LSD was used. One sample t-test with a hypothetical value of 100 % was applied when given specific binding values were compared to total specific binding (100 %) in receptor binding assays. Statistical analysis was performed with GraphPad Prism 7.0 program; significance was accepted at $P < 0.05$ level.

3 RESULTS

3.1 KYNA does not show direct binding to the CB₁R, does not induce G-protein activation nor does it alter CB₁R ligand binding or CB₁R-mediated G-protein stimulation

To study the binding affinity of KYNA to CB₁Rs, competition binding experiments were performed in rat whole brain membranes using [³H]WIN55,212-2, a non-selective cannabinoid radioligand. [³H]WIN55,212-2 showed adequate binding properties on the applied membrane homogenates, reaching a 3.3 nM K_i value in homologous displacement (Table 1, Fig. 2A). [³H]WIN55,212-2 in the brain preferably binds to CB₁Rs, which is supported by our results where the CB₂R selective agonist CB65 reduced the total specific binding of [³H]WIN55,212-2 significantly less effectively compared to the CB₁R selective ACEA (Table 1, Fig. 2A). For comparison 10 μM CB65 reduced total specific binding of the radioligand to 60 %, whereas in the presence of ACEA total specific binding reached the non-specific binding level (0 %, Table 1, Fig. 2A).

KYNA on its own did not alter significantly the specific binding of the radioligand, indicating the lack of specific affinity towards the CB₁R. When KYNA was added in 10 μM to ACEA, no horizontal shifts were observed in the concentration curves of the compound, indicating the lack of allosteric modulation.

G-protein activity measurements were achieved using [³⁵S]GTPγS binding assays also in rat whole brain membranes. In the presence of KYNA in the applied concentration range, [³⁵S]GTPγS specific binding was unaltered, remaining in the basal activity level (Fig. 2B, Table 1.). For comparison the CB₁R full agonist ACEA concentration dependently increased [³⁵S]GTPγS specific binding with a maximum effectivity (E_{max}) of 170.2 % and a potency (EC₅₀) of 137.8 nM (Table 1, Fig. 2B). Additionally, these parameters were not altered in the presence of 10 μM KYNA (Table 1, Fig. 2B).

Table 1. CB₁R affinity (K_i) and CB₁R-mediated G-protein efficacy (E_{max}) and ligand potency (EC_{50}) values of KYNA and the CB₁R selective ACEA alone and in combination with KYNA. K_i values of the non-selective CBR ligand WIN55,212-2 and the CB₂R selective CB65 ligand is also indicated for control and for comparison. The indicated parameters were calculated from the concentration-effect curves presented in Figure 2A (K_i) and B (E_{max} , EC_{50}) and were statistically analyzed as discussed in section 2.5.

Compounds	CB ₁ R affinity ([³ H]WIN55,212-2 binding)		G-protein activity ([³⁵ S]GTP γ S binding)		
	$K_i \pm S.E.M.$ (nM)	n	$E_{max} \pm S.E.M.$ (%)	$EC_{50} \pm S.E.M.$ (nM)	n
KYNA	not relevant ¹	4	100.9 \pm 1.22	not relevant ¹	3
ACEA	202.9 \pm 55.28	4	170.2 \pm 6.55	137.72 \pm 53.22	3
ACEA + 10 μ M KYNA	214.92 \pm 40.26	4	164.4 \pm 6.43	129.12 \pm 52.55	3
WIN55,212-2	3.74 \pm 0.89	4	N.D.		
CB65	>1000	4	N.D.		

¹: Total specific binding (100%) was not altered significantly (one-sample t test with 100 % theoretical value), thus K_i value calculation is not relevant

²: [³H]WIN55,212-2 binding was only reduced to 62 %.

N.D.: not determined.

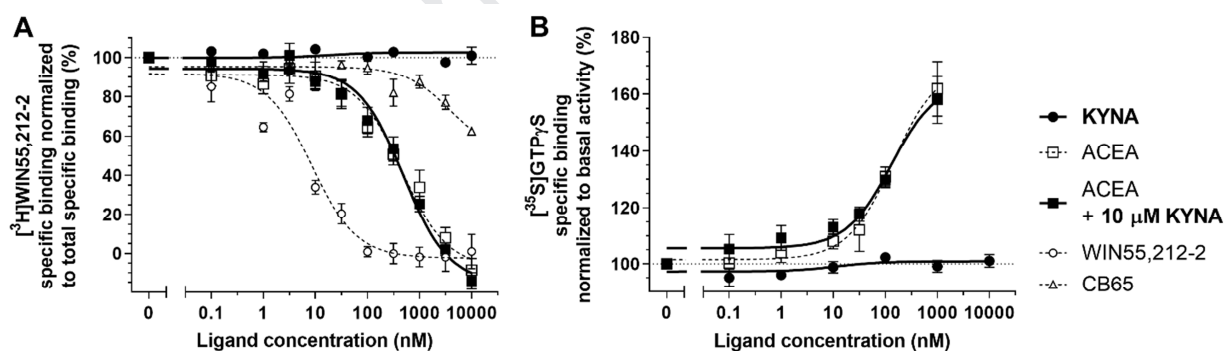


Figure 2. CB₁R binding affinity (A) and G-protein activity (B) of KYNA and the CB₁R selective ACEA in the presence or absence of KYNA in concentration-response binding curves of [³H]WIN55,212-2 competition and functional [³⁵S]GTP γ S binding assays. Assays were performed in rat brain membrane homogenates. Figures represent the specific binding of [³H]WIN55,212-2 or [³⁵S]GTP γ S in percentage (means \pm S.E.M.) normalized to total specific binding (100 %, which equals to basal activity in case of G-protein activity) in the presence of increasing concentrations of KYNA (0.1 nM - 10 μ M), ACEA (A: 0.1 nM - 10 μ M; B: 0.1 nM - 1 μ M), WIN55,212-2 or CB65 (0.1 nM - 10 μ M). ACEA binding and G-protein activity was also measured in the presence of 10 μ M KYNA. Total specific binding was measured in the absence of the indicated compounds. Dotted lines represent total specific binding (A) or basal activity level (B). Curve parameters (A: K_i ; B: E_{max} , EC_{50}) are indicated in Table 1. Curves were fitted as described in section 2.5, binding assays were performed according to section 2.3.2 and 2.3.3.

3.2 Chronic systemic KYNA treatment increases the KYNA CSF and plasma levels

In order to investigate whether our applied treatment condition allows the KYNA to enter the CNS, we measured the KYNA concentration in the CSF and also in the plasma for comparison. The plasma KYNA levels significantly increased as expected (Table 2). More interestingly, KYNA CSF levels also increased following the treatment (Table 2), although the concentration levels in both groups were significantly lower as compared to the plasma levels (Table 2). This indicates the limited BBB penetration of KYNA. For reference, plasma and CSF concentrations of other metabolites of the KP were also measured, namely L-KYN and tryptophan. Neither of them showed significant difference following the treatment (Table S1).

Table 2. KYNA concentration levels in plasma and CSF following systemic KYNA chronic treatment (i.p., 9 days, 128 mg/kg/day). Experiments were analyzed and performed as described in section 2.5 and 2.4, respectively.

Plasma		CSF	
Concentration \pm S.E.M. (nM)		Concentration \pm S.E.M. (nM)	
Vehicle	KYNA	Vehicle	KYNA
63.95 \pm 7.95 (n=5)	307.58 \pm 60.44** (n=5)	3.32 \pm 1.32 ^{###} (n=5)	10.69 \pm 2.04* ^{/##} (n=4)

*: indicates the significant difference compared to vehicle (unpaired t test, two-tailed P value).

#: indicates the significant difference compared to their corresponding group measured in the plasma (unpaired t test, two-tailed P value).

3.3 Chronic systemic KYNA treatment significantly increases the amount of CB₁R-coupled G-proteins in rat whole brain, without affecting the efficacy and the potency of the receptor and selective ligands, respectively

In our further experiments the long-term effect of systemic KYNA treatment on CB₁R-mediated G-protein activity was investigated in [³⁵S]GTP γ S binding assays in rat whole brain membranes (excluding the cerebellum). CB₁R was initially stimulated by the CB₁R selective agonist ACEA in increasing concentrations (Fig. 3). In the vehicle treated group, as expected ACEA concentration dependently increased the level of [³⁵S]GTP γ S specifically bound to CB₁R-coupled G-protein as compared to total specifically bound [³⁵S]GTP γ S or to basal activity level (Table 3, Fig. 3A). The same tendency was observed in the KYNA treated group, however, the basal activity level significantly increased in these samples, as well as the amount of [³⁵S]GTP γ S specifically bound to CB₁R-coupled G-protein in the individual concentration points (Fig. 3A, Table 3). The amount of maximally stimulated (E_{max}) CB₁R-coupled G-proteins also significantly increased compared to the vehicle (Table 3). Importantly, the non-specific binding level of [³⁵S]GTP γ S did not change significantly between the two groups, which confirms their unaltered overall protein content (Table 3).

To examine whether the overall performance of ACEA was also changed significantly after the treatment, data was normalized to basal activity levels of G-proteins (100 %, Fig. 3B). The maximum efficacy and the ligand potency (EC_{50}) of the agonist ACEA was significantly not different (Table 3, Fig. 3B), indicating that although the amount of available CB₁R-coupled G-proteins increased in the brain, the overall performance of the ligand and the activity of CB₁R-coupled G-proteins remained the same.

To support our results, we applied another CB₁R selective ligand, namely the highly selective inverse agonist rimonabant. As expected, rimonabant concentration dependently decreased the specifically bound [³⁵S]GTP γ S to CB₁R-coupled G-protein compared to basal activity. With rimonabant, we obtained the same results as with ACEA, namely the amount of G-proteins and CB₁R-coupled G-proteins in both basal activity and maximal efficacy, respectively, significantly increased due to the KYNA treatment. These changes did not alter significantly the overall performance of the ligand similar to ACEA (Table 3, Fig. 3B). As expected, the basal activity and non-specific binding levels in vehicle and KYNA treated groups did not differ

significantly between rimonabant and ACEA (Table 3), which also validated the experimental set up.

Table 3. The effect of long-term systemic KYNA treatment (i.p., 9 days, 128 mg/kg/day) compared to vehicle on CB₁R-coupled G-protein activity in rat brain membranes described by the indicated parameters obtained from [³⁵S]GTPγS binding assays. CB₁R was stimulated by the highly CB₁R selective agonist ACEA and inverse agonist rimonabant. The table highlights the non-specific binding (*NS*), basal activity (*Basal*) and maximum efficacy (*E_{max}*) levels of CB₁R-coupled G-protein activity upon receptor stimulation given in specifically bound [³⁵S]GTPγS of protein content. *E_{max}* levels and ligand potency (*EC₅₀*) values were also calculated when data were normalized to basal activity levels (100 %) to see the overall performance of the ligands. Data were obtained from concentration-effect curves shown in Fig. 3 and statistically analyzed based on section 2.5.

Compounds	Treatment (n)	Normalized to protein content			Normalized to basal activity	
		<i>NS</i> ± S.E.M. (fmol/mg)	<i>Basal</i> ± S.E.M. (fmol/mg)	<i>E_{max}</i> ± S.E.M. (fmol/mg)	<i>E_{max}</i> ± S.E.M. (%)	<i>EC₅₀</i> ± S.E.M. (nM)
ACEA	Vehicle (5)	19.89 ± 1.89	40.43 ± 8.52	61.76 ± 14.57	153.3 ± 6.99	1059.25 ± 626.93
	KYNA (8)	23.77 ± 1.39	85.18 ± 13.12*	124 ± 15.95*	152.6 ± 5.6	1713.96 ± 902.28
Rimonabant	Vehicle (7)	20.6 ± 1.13	50.56 ± 2.85	12.1 ± 3.78	14.8 ± 6.86	1870.68 ± 601.76
	KYNA (7)	22.92 ± 1.55	81.73 ± 2.74***	26.6 ± 4.41*	27.91 ± 4.74	2004.47 ± 478.91

*: significant difference compared to vehicle treated (unpaired t test, two-tailed P value; *: P < 0.05; ***: P < 0.001

NS: non-specific binding

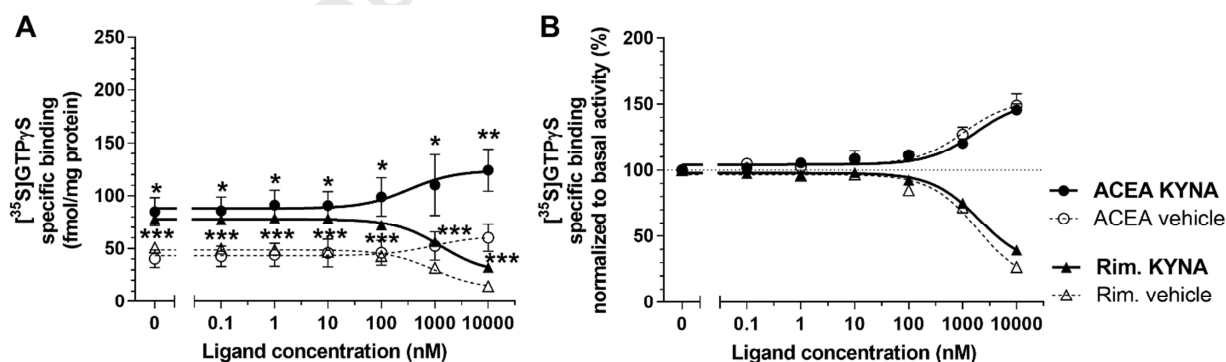


Figure 3. The effect of long-term systemic KYNA treatment (i.p., 9 days, 128 mg/kg/day) on CB₁R-coupled G-protein activity compared to vehicle in rat brain membranes depicted in concentration-effect curves of [³⁵S]GTPγS binding assays. CB₁R was stimulated by the highly CB₁R selective agonist ACEA and inverse agonist rimonabant (*Rim.*). Figures represent the specifically bound [³⁵S]GTPγS of protein in fmol/mg (A) or in percentage normalized to basal activity levels (100 %) (B) in the presence of increasing concentrations (0.1 nM-10μM) of ACEA or rimonabant. Data are presented as means ± S.E.M. Basal activity levels were determined in the absence of the indicated ligands. Dotted line indicates basal activity levels. * indicates the significant difference of individual concentration points between vehicle and KYNA

treated samples (two-way ANOVA, uncorrected Fisher's LSD; *: $P < 0.05$; **: $P < 0.01$; ***: $P < 0.001$). Data were fitted as described under section 2.5, assays were performed as discussed in section 2.3.3.

3.4 Chronic systemic KYNA treatment enhances the CB₁R maximum binding capacity in rat whole brain without altering the binding affinity of the receptor

In the next step, we examined whether the number of CB₁R binding sites also increased apart from the amount of CB₁Rs coupled to the G-protein in rat whole brain following chronic systemic KYNA treatment. Saturation binding experiments were conducted using [³H]WIN55,212-2 radioligand to detect CB₁R binding sites by applying the radioligand in increasing concentration to saturate the binding sites of the receptors. In vehicle treated samples the amount of [³H]WIN55,212-2 specifically bound to CB₁Rs concentration dependently increased and reached saturation, which renders the maximum binding capacity (B_{\max}) or the density of the receptor (Fig. 4, Table 4). The KYNA treatment significantly increased the amount of specifically bound radioligand to the receptor protein from 4.17 nM compared to vehicle treatment (Fig. 4). As a result, in the KYNA treated group the plateau value of the saturation curve significantly increased, compared to vehicle group, which indicated a significantly higher B_{\max} value and thus higher receptor density (Fig. 4, Table 4). However, the affinity of the radioligand (equilibrium dissociation constant, K_d), did not change significantly (Table 4). In both samples, the non-specific binding level of the radioligand concentration dependently and linearly increased, as expected (inset of Fig. 4). Additionally, the slope of the linear regression quantifying the non-specific binding level did not change significantly (vehicle: 27.84 ± 1.07 vs. KYNA: 28.53 ± 0.83), which also validates the equivalent protein content of the two sample groups.

These data, together with the G-protein activity measurements, indicates that the amount of CB₁Rs binding sites and CB₁Rs coupled to the G-protein increased as a result of chronic KYNA treatment, without affecting the stimulatory or ligand binding of the receptor.

Table 4. The effect of long-term systemic KYNA treatment (i.p., 9 days, 128 mg/kg/day) on CB₁R maximum binding capacity (B_{max}) and binding affinity (dissociation constant; K_d) in saturation binding assays using [³H]WIN55,212-2 radioligand to detect CB₁Rs in rat brain membranes. Data were obtained and analyzed from concentration-effect curves presented in Fig. 4 as described in section 2.5.

Treatment (n)	[³ H]WIN55,212-2 saturation binding	
	$B_{max} \pm S.E.M.$ (fmol/mg)	$K_d \pm S.E.M.$ (nM)
Vehicle (4)	1339.25 \pm 54.79	9.17 \pm 1.04
KYNA (4)	1879.09 \pm 54.44***	11.69 \pm 0.91

*: significant difference compared to vehicle treated (unpaired t test, two-tailed P value; ***: P < 0.001)

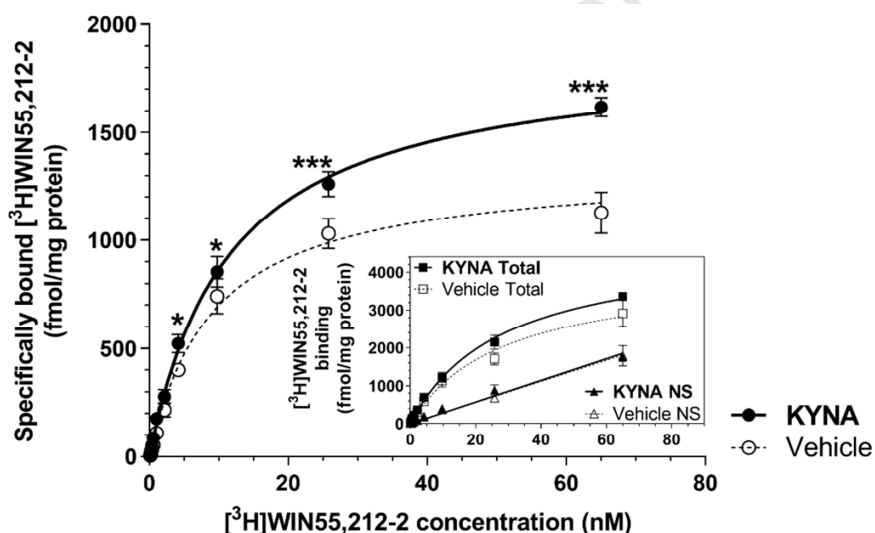


Figure 4. The effect of long-term systemic KYNA treatment (i.p., 9 days, 128 mg/kg/day) on CB₁R binding capacity and affinity compared to vehicle in rat brain membranes depicted in concentration-effect curves of [³H]WIN55,212-2 saturation binding assays. Figure represents the specific binding (inset figure: total and non-specific binding; indicated as 'Total' and 'NS') of the radioligand in the presence of increasing concentration (0.13 - 65 nM) of the applied radioligand in vehicle and KYNA treated groups. * indicates the significant difference of individual concentration points between vehicle and KYNA treated samples (two-way ANOVA, uncorrected Fisher's LSD; *: P < 0.05; ***: P < 0.001). Data are presented as means \pm S.E.M. and were fitted as described in section 2.5. Saturation binding assays were performed as discussed in section 2.3.4.

3.5 Chronic systemic KYNA treatment significantly increases the amount of CB₁R-coupled G-proteins in rat hippocampus, but not in the cortex and brainstem

In the following experiments, we further investigated the brain region specificity of the obtained G-protein activity results from whole brain. Three main regions relevant to CB₁R expression and function were chosen: cortex, hippocampus and brainstem. To detect CB₁Rs only the agonist ACEA was used. It was found that compared to the vehicle group only the hippocampus displayed elevated levels of G-protein coupled CB₁Rs, whereas in the cortex and brainstem its abundance remained unaltered (Fig. 5, Table 5). Similarly to the whole brain, the basal activity, the levels of ACEA-induced specifically bound [³⁵S]GTPγS and the amount of maximum ACEA-stimulated G-protein coupled CB₁Rs in the hippocampus was significantly enhanced as compared to the vehicle treated group (Fig. 5B, Table 5). The potency of the agonist ligand, as well as the maximum efficacy of the stimulated G-protein did not change significantly in the KYNA and vehicle treated groups (Fig. 5E, Table 5). Similar findings were observed in the cortex and brainstem too (Fig 5B and F, Table 5). The non-specific binding levels remained unaltered following the treatment in all three brain regions (Table 5).

Table 5. The effect of long-term systemic KYNA treatment (i.p., 9 days, 128 mg/kg/day) compared to vehicle on CB₁R-coupled G-protein activity in rat cortex, hippocampus and brainstem described by the indicated parameters obtained from [³⁵S]GTPγS binding assays. CB₁R was stimulated by the highly CB₁R selective agonist ACEA in increasing concentrations. The table highlights the non-specific binding (*NS*), basal activity (*Basal*) and maximum efficacy (*E_{max}*) levels of CB₁R-coupled G-protein activity upon receptor stimulation given in specifically bound [³⁵S]GTPγS of protein content. *E_{max}* levels and ligand potency (*EC₅₀*) values were also calculated when data were normalized to basal activity levels (100 %) to see the overall performance of the ligand. Data were obtained from concentration-effect curves shown in Fig. 5 and statistically analyzed based on section 2.5.

<i>Brain region</i>	<i>Treatment (n)</i>	Normalized to protein content			Normalized to basal activity	
		<i>NS</i> ± <i>S.E.M.</i> (fmol/mg)	<i>Basal</i> ± <i>S.E.M.</i> (fmol/mg)	<i>E_{max}</i> ± <i>S.E.M.</i> (fmol/mg)	<i>E_{max}</i> ± <i>S.E.M.</i> (%)	<i>EC₅₀</i> ± <i>S.E.M.</i> (nM)
Cortex	Vehicle (3)	5.53 ± 0.18	60.09 ± 6.28	96.03 ± 12.69	159.8 ± 5.92	189.23 ± 74.34
	KYNA (3)	5.47 ± 0.03	61.28 ± 3.39	97.96 ± 7.19	160.2 ± 6.4	243.22 ± 97.66
Hippocampus	Vehicle (6)	6.49 ± 0.44	84.7 ± 6.45	161.7 ± 8.71	193.1 ± 4.56	130.32 ± 24.69
	KYNA (5)	7.42 ± 0.25	119.5 ± 4.46**	217.3 ± 11.93**	186.7 ± 6.28	161.81 ± 38.66
Brainstem	Vehicle (6)	9.91 ± 3.02	26.34 ± 2.84	36.39 ± 4.17	129.8 ± 1.92	91.41 ± 20.23
	KYNA (4)	9.91 ± 4.49	26.52 ± 6.73	33.18 ± 9.55	130.3 ± 1.92	96.16 ± 22.88

*: significant difference compared to vehicle treated (unpaired t test, two-tailed P value; **: P < 0.01)

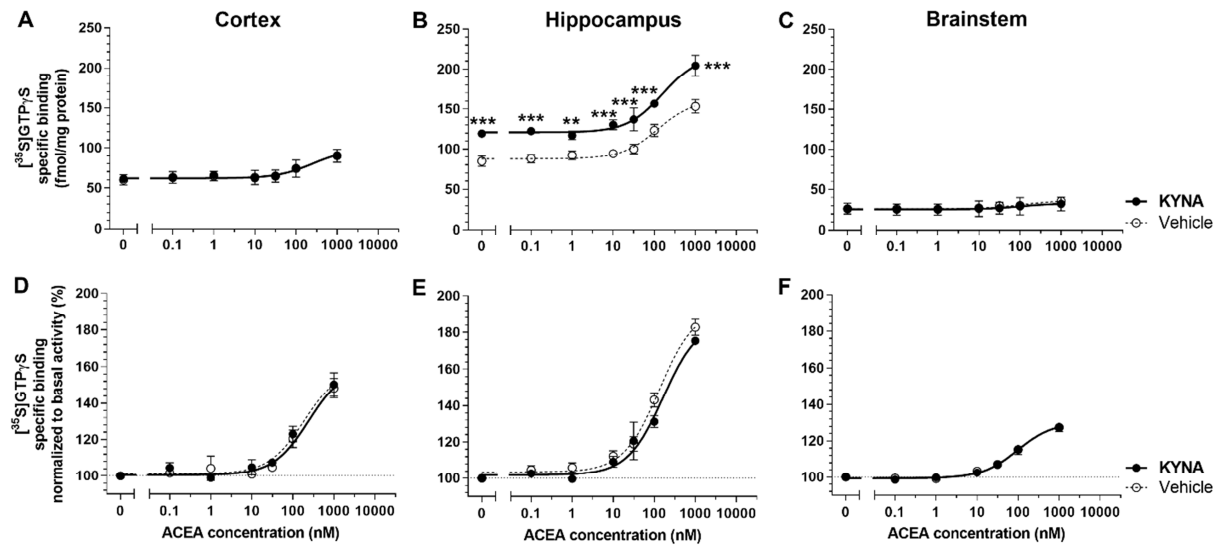


Figure 5. The effect of long-term systemic KYNA treatment (i.p., 9 days, 128 mg/kg/day) on CB₁R-coupled G-protein activity compared to vehicle in rat cortex (A and D), hippocampus (B and E) and in brainstem (C and F) depicted in concentration-effect curves of [³⁵S]GTPγS binding assays. CB₁R was stimulated by the highly CB₁R selective agonist ACEA. Figures represents the specifically bound [³⁵S]GTPγS of protein in fmol/mg (A-C) or in percentage normalized to basal activity levels (100%) (D-F) in the presence of increasing concentrations (0.1 nM - 10 μM) of ACEA. Data are presented as means ± S.E.M. Basal activity levels were determined in the absence of the indicated ligands. Dotted line represents basal activity levels. * indicates the significant difference of individual concentration points between vehicle and KYNA treated samples (two-way ANOVA, uncorrected Fisher's LSD; **: P < 0.01; ***: P < 0.001). Data were fitted as described under section 2.5, assays were performed as discussed in section 2.3.3.

3.6 Chronic systemic KYNA treatment enhances the CB₁R maximum binding capacity in rat hippocampus without altering the binding affinity of the receptor

To support our G-protein activity measurements in the hippocampus, we performed saturation binding assays in order to examine the maximum binding capacity of CB₁Rs in this brain region. The experimental setup was the same as described in section 3.4.

It was found that the KYNA treatment - as similarly seen in the whole brain - significantly increased the maximum binding capacity of the CB₁Rs in the hippocampus, indicating a higher number of CB₁R binding sites in this brain region of this group (Table 6. and Fig. 6). The K_d value of the radioligand did not change significantly, as well as the non-specific binding level, indicated by the significantly unaltered slope (Vehicle: 50.10 ± 1.25 vs. 52.34 ± 0.84 ; inset Fig. 6).

Table 6. The effect of long-term systemic KYNA treatment (i.p., 9 days, 128 mg/kg/day) in rat hippocampus on CB₁R maximum binding capacity (B_{max}) and binding affinity (dissociation constant; K_d) in saturation binding assays using [³H]WIN55,212-2 radioligand to detect CB₁Rs. Data were obtained and analyzed from concentration-effect curves presented in Fig. 6 as described in section 2.5.

Treatment (n)	[³ H]WIN55,212-2 specific binding	
	$B_{max} \pm S.E.M. (fmol/mg)$	$K_d \pm S.E.M. (nM)$
Vehicle (4)	1069.16 \pm 96.83	13.39 \pm 2.98
KYNA (4)	1403.23 \pm 75.36*	16.74 \pm 2.07

*: significant difference compared to vehicle treated (unpaired t test, two-tailed P value)

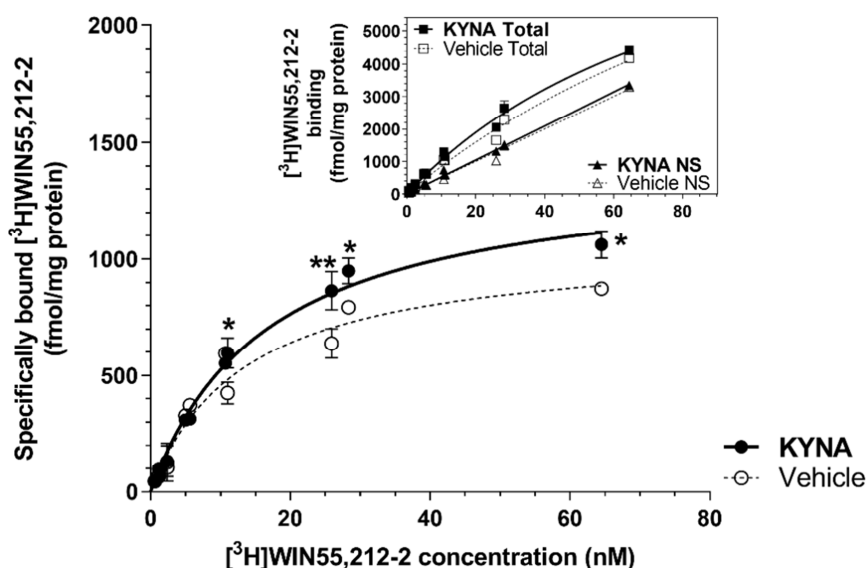


Figure 6. The effect of long-term systemic KYNA treatment (i.p., 9 days, 128 mg/kg/day) in rat hippocampus on CB₁R binding capacity and affinity compared to vehicle depicted in concentration-effect curves of [³H]WIN55,212-2 saturation binding assays. Figures represent the specific binding (inset figure: total and non-specific binding; indicated as 'Total' and 'NS') of the radioligand in the presence of increasing concentration (0.59 - 64.5 nM) of the applied radioligand in vehicle or KYNA treated groups. * indicates the significant difference of individual concentration points between vehicle and KYNA treated samples (two-way ANOVA, uncorrected Fisher's LSD; *: $P < 0.05$; **: $P < 0.01$). Data are presented as means \pm S.E.M. and were fitted as described in section 2.5. Saturation binding assays were performed as discussed in section 2.3.4.

4 DISCUSSION

A special attention has been given recently to the overlapping elements of the KP and the ECS and this field has been reviewed by our group and by others previously (Colín-González et al., 2016; Nagy-Grócz et al., 2017; Zádor et al., 2019). Our study focuses on two significant components of the KP and the ECS, the KYNA and the CB₁R, respectively. Both elements are widely present throughout the body, however, the brain is where they have prominent roles and are most studied. In this work, we found for the first time, that enhanced CSF KYNA levels induced by systemic long-term KYNA treatment increased the abundance of functional CB₁R in whole brain, which is also manifested in the hippocampus. Importantly, this effect was indirect, as KYNA did not show affinity towards the CB₁R.

One of the key initial points of our current work was the well-known fact that KYNA is an endogenous agonist ligand for GPCR35, which similarly to the CB₁R belong to the GPCR family and activates G_{i/o}-mediated signaling (Demuth and Molleman, 2006; Guo et al., 2007; Ohshiro et al., 2008; Wang et al., 2006). Thus, it was intriguing to examine the binding and receptor activation capabilities of KYNA to the CB₁R. Based on our binding studies KYNA did not bind directly to the CB₁R, furthermore it did not alter the affinity of the CB₁R specific ligand, ACEA. To examine the receptor activation (agonist, inverse agonist or antagonist) properties of KYNA on the receptor, we applied [³⁵S]GTPγS binding assays. As mentioned in section 2.3.3, our experimental protocol is optimized for monitoring G_{i/o}-type G-proteins (DeLapp et al., 2004), which G-protein type is also stimulated by KYNA via GPR35 (Milligan, 2011; Wang et al., 2006). Accordingly, agonist-stimulated CB₁R coupled G-protein activity was unaltered in the presence of KYNA and the monitored G-proteins were not stimulated when only KYNA was present. These data, together with our receptor binding affinity results confirms that KYNA does not interact directly with the CB₁R. Worthy of note, G-protein activity was measured in rat brain, where GPR35 receptors are sparsely expressed (Taniguchi et al., 2006), which is why we did not observe KYNA-stimulated GPR35 coupled G-protein activation in our samples. Additionally, the difference in the amino acid residues that form the binding pocket and that are responsible for agonist binding of CB₁R and GPR35 (Krishna Kumar et al., 2019; Milligan, 2011; Zhao et al., 2014) may explain why KYNA did not bind to the CB₁R. Similar to other class A GPCRs, the binding pocket of CB₁R and GPR35 is formed by almost the same transmembrane helix domains (3; 6 and 7) (Krishna Kumar et al., 2019; Milligan, 2011; Venkatakrishnan et al., 2013; Zhao et

al., 2014). However, compared to other GPCRs the agonist binding pocket of CB₁R is further buried in the transmembrane domains of the receptor (Krishna Kumar et al., 2019), which may also contribute to the inability of KYNA to interact with the orthosteric binding site of the receptor.

Previously our study demonstrated that systemic, high dose (128 mg/kg/day) long-term (9 days) KYNA administration altered opioid receptor G-protein activity without directly binding to the receptor (Zádor et al., 2014b). Since cannabinoid and opioid receptors also share many features - including G_{i/o} type G-protein signaling and structure (Christie, 2006; Viganò et al., 2005) - we investigated the effect of the same KYNA treatment on the CB₁R. Before this, we examined whether the long-term systemic KYNA treatment altered brain (CSF) KYNA levels. KYNA – despite its relatively limited access to the CNS (Fukui et al., 1991) - can elicit central effects when administered systemically in large doses (Gill and Woodruff, 1990; Scharfman and Goodman, 1998) and can also increase the normally low nanomolar endogenous brain KYNA levels to micromolar concentration levels (Wu et al., 2000). Indeed, the applied dose of KYNA in our experiments was high, (128 mg/kg) and it significantly enhanced KYNA CSF levels compared to control. As expected, plasma KYNA levels also increased after the treatment. Plasma and CSF KYNA levels in the vehicle treated group corresponded well with previous data (Wu et al., 2000).

With the [³⁵S]GTPγS binding assay we monitored CB₁R-mediated G-protein activity, firstly in the whole brain of the rats, excluding the cerebellum to have an overall view of the effect of KYNA on central CB₁Rs. This larger brain structure contains the cortex, hippocampus and brainstem. Our hypothesis was that in case we observe KYNA-induced alterations in CB₁Rs in this structure, we would further analyze the brain region specificity of the effect in the cortex, hippocampus and brainstem, which are relevant regions for CB₁R function and expression (see later on). According to our data, KYNA administered in 128 mg/kg/day, i.p. after 9 days did not alter significantly the G-protein maximal efficacy nor the agonist ligand potency mediated via CB₁R. Interestingly, in our previous study with opioid receptors the same treatment induced significant changes in these parameters brain region and opioid receptor type specifically (Zádor et al., 2014b). However, the amount of G-proteins at basal activity level significantly increased and so did the levels of CB₁R coupled G-proteins, including those, which displayed maximum efficacy. This was observed both upon CB₁R selective agonist and inverse agonist stimulation,

which concentration dependently increased and decreased G-protein basal activity, respectively (Kenakin, 2001). Since the protein levels of CB₁R coupled G-proteins enhanced upon the treatment, the next step was to assess the amount of CB₁R binding sites in saturation binding assays - from which the maximum binding capacity of the receptor can be analyzed. Accordingly, not only the amount of CB₁R coupled G-proteins increased but the density (maximum binding capacity) of the CB₁R as well. Furthermore, the ligand binding of the receptor was not affected significantly by the treatment, and since binding affinity affects ligand potency, these results correspond well with the G-protein activity measurements, where ligand potency also remained unchanged. Thus, overall we can conclude that long-term KYNA treatment significantly increased the abundance of functional CB₁Rs in the brain, without affecting the receptor binding and stimulation properties.

In the next step, we analyzed the brain region specificity of the observed results. We chose the cortex, hippocampus and brainstem areas for multiple reasons. The cortex and brainstem covers significant areas of the rat whole brain, additionally the cortex region is rich in CB₁Rs in contrast to the brainstem (Herkenham et al., 1990; Mackie, 2005). However, the brainstem - similarly to the cortex - mediate important functions relevant to CB₁Rs, such as energy regulation, food intake and they are involved in certain psychiatric disorders too (Cota et al., 2006; Desfossés et al., 2010). Despite the small dimensions of the rat hippocampus, it is one of the most densely populated brain region in terms of CB₁Rs (Herkenham et al., 1990; Mackie, 2005). Hippocampal CB₁Rs for example have a significant role in cognitive functions (Pacher et al., 2006). Therefore, in our further experiments we applied G-protein activity measurements in the brain areas of our interest. With the same experimental setup, only the hippocampus showed the same changes as it was found in the whole brain. The amount of CB₁R coupled G-proteins remained unaltered in the cortex and brainstem. Furthermore, in all brain regions the G-protein maximum stimulation and the potency of the applied selective ligand showed no significant alteration. These results were further confirmed by saturation binding assays in the hippocampus, where the density of CB₁Rs also significantly increased following the treatment, whereas the binding property of the receptor did not differ significantly in KYNA and vehicle treated samples. Additionally, in the investigated brain regions the level of specifically bound [³⁵S]GTPγS and cannabinoid radioligand correlated well with earlier studies (Berrendero et al., 2003; Mackie, 2005). Worthy of note, that hippocampus samples were only homogenized and no

membrane fractions were prepared from them. This was necessary due to the small size of the brain region and also to limit the number of sacrificed animals for the assays. Nevertheless, the non-specific binding levels remained unaltered both in vehicle and KYNA treated samples, indicating that the overall protein content was the same. The receptor up-regulation seen in the whole brain was not entirely reflected by the changes observed in the hippocampus, most probably because other regions are involved apart from cortex, and brainstem, which can be potentially explored in a future study. Additionally, KYNA levels were also measured in the cortex, hippocampus and brainstem and we found no difference between vehicle and KYNA treated group (Table S2). Similar results were observed with L-KYN and tryptophan (Table S2).

One possible explanation for the up-regulation of brain CB₁Rs can be a compensatory mechanism or neuroadaptation triggered by the long-term KYNA treatment. Such mechanisms in the brain have been previously proposed in certain conditions such as in rats withdrawn from palatable food cycling (Blasio et al., 2013), in patients with anorexia nervosa (Gérard et al., 2011) or posttraumatic stress disorder (Neumeister et al., 2015). Moreover, alterations in the ECS has been described in nearly all classes of diseases, and in certain pathological conditions CB₁R up-regulation can be protective as well as maladaptive (Miller and Devi, 2011). Brain KYNA levels can also be elevated in multiple neurological related disorders, which can either be neuroprotective or neurotoxic (Párdutz et al., 2012; Szalardy et al., 2012; Varga et al., 2015; Vécsei et al., 2013; Zádori et al., 2011a, 2011b). Regarding our study, schizophrenia is particularly interesting, since patients suffering from such psychiatric disorder show elevated KYNA levels in the CSF and increased CB₁R density in the brain (Erhardt et al., 2017; Ibarra-Lecue et al., 2018). It is assumed that elevated endogenous brain KYNA level is a persistent condition in the brains of patients with schizophrenia (Nilsson et al., 2006), therefore we hypothesize that such permanent state may also evoke CB₁R up-regulation - as we saw in our results - as a compensatory mechanism. Such hypothesis will be further investigated thoroughly by our group in the near future.

5 SUMMARY AND CONCLUSIONS

In this study, we excluded for the first time the direct binding of KYNA to the CB₁R. Moreover, we also found for the first time that long-term systemic high dose KYNA treatment enhanced the amount of functional CB₁R binding sites in the whole brain, without affecting the overall activity and ligand binding of the receptor. Similar results were obtained from a more specific brain region, namely the hippocampus. The applied treatment also elevated KYNA levels in the CSF, indicating that KYNA is involved indirectly in the observed effects. These findings might reveal a possible connection between high KYNA CSF levels and increased brain CB₁R density characterized by schizophrenia.

DECLARATION OF INTEREST

There are none.

FUNDING

This study was supported by the Economic Development and Innovation Operational Programme (grant number GINOP 2.3.2-15-2016-00034) and by the Ministry of Human Capacities, Hungary (grant number 20391-3/2018 FEKUSTRAT). Cs.T. and Sz.D. were supported by the National Research, Development and Innovation Office (grant number K124952) and by the Economic Development and Innovation Operational Programme (GINOP-2.3.2-15-2016-00060). Cs.E.K. was supported by the New National Excellence Program of the Ministry for Innovation and Technology (grant number UNKP-19-3) and by the “Young researchers from talented students” project (grant number EFOP-3.6.3-VEKOP-16-2017-00009).

REFERENCES

- Beggiato, S., Ieraci, A., Tomasini, M.C., Schwarcz, R., Ferraro, L., 2020. Prenatal THC exposure raises kynurenic acid levels in the prefrontal cortex of adult rats. *Prog. Neuro-Psychopharmacology Biol. Psychiatry* 100, 109883. <https://doi.org/10.1016/J.PNPBP.2020.109883>
- Beggiato, S., Tanganelli, S., Fuxe, K., Antonelli, T., Schwarcz, R., Ferraro, L., 2014. Endogenous kynurenic acid regulates extracellular GABA levels in the rat prefrontal cortex. *Neuropharmacology* 82, 11–18. <https://doi.org/10.1016/j.neuropharm.2014.02.019>
- Benyhe, S., Farkas, J., Tóth, G., Wollemann, M., 1997. Met5-enkephalin-Arg6-Phe7, an endogenous neuropeptide, binds to multiple opioid and nonopioid sites in rat brain. *J. Neurosci. Res.* 48, 249–58.
- Berrendero, F., Mendizabal, V., Murtra, P., Kieffer, B.L., Maldonado, R., 2003. Cannabinoid receptor and WIN 55 212-2-stimulated [35S]-GTPgammaS binding in the brain of mu-, delta- and kappa-opioid receptor knockout mice. *Eur. J. Neurosci.* 18, 2197–2202. <https://doi.org/10.1046/j.1460-9568.2003.02951.x>
- Birch, P.J., Grossman, C.J., Hayes, A.G., 1988. Kynurenate and FG9041 have both competitive and non-competitive antagonist actions at excitatory amino acid receptors. *Eur. J. Pharmacol.* 151, 313–5.
- Blasio, A., Iemolo, A., Sabino, V., Petrosino, S., Steardo, L., Rice, K.C., Orlando, P., Iannotti, F.A., Di Marzo, V., Zorrilla, E.P., Cottone, P., 2013. Rimonabant precipitates anxiety in rats withdrawn from palatable food: role of the central amygdala. *Neuropsychopharmacology* 38, 2498–507. <https://doi.org/10.1038/npp.2013.153>
- Bortz, D.M., Wu, H.-Q., Schwarcz, R., Bruno, J.P., 2017. Oral administration of a specific kynurenic acid synthesis (KAT II) inhibitor attenuates evoked glutamate release in rat prefrontal cortex. *Neuropharmacology* 121, 69–78. <https://doi.org/10.1016/j.neuropharm.2017.04.023>
- Carrillo-Mora, P., Méndez-Cuesta, L.A., Pérez-De La Cruz, V., Fortoul-van Der Goes, T.I., Santamaría, A., 2010. Protective effect of systemic L-kynurenine and probenecid administration on behavioural and morphological alterations induced by toxic soluble

- amyloid beta (25-35) in rat hippocampus. *Behav. Brain Res.* 210, 240–50.
<https://doi.org/10.1016/j.bbr.2010.02.041>
- Chen, Y., Brew, B.J., Guillemin, G.J., 2011. Characterization of the kynurenine pathway in NSC-34 cell line: implications for amyotrophic lateral sclerosis. *J. Neurochem.* 118, 816–25.
<https://doi.org/10.1111/j.1471-4159.2010.07159.x>
- Cheng, Y., Prusoff, W.H., 1973. Relationship between the inhibition constant (K₁) and the concentration of inhibitor which causes 50 per cent inhibition (I₅₀) of an enzymatic reaction. *Biochem. Pharmacol.* 22, 3099–108.
- Christie, M.J., 2006. Opioid and cannabinoid receptors: friends with benefits or just close friends? *Br. J. Pharmacol.* 148, 385–386. <https://doi.org/10.1038/sj.bjp.0706756>
- Colín-González, A.L., Aguilera, G., Santamaría, A., 2016. Cannabinoids: Glutamatergic Transmission and Kynurenines, in: *Advances in Neurobiology*. pp. 173–198.
https://doi.org/10.1007/978-3-319-28383-8_10
- Cota, D., Tschöp, M.H., Horvath, T.L., Levine, A.S., 2006. Cannabinoids, opioids and eating behavior: the molecular face of hedonism? *Brain Res. Rev.* 51, 85–107.
<https://doi.org/10.1016/j.brainresrev.2005.10.004>
- Cseh, E.K., Veres, G., Szentirmai, M., Nánási, N., Szatmári, I., Fülöp, F., Vécsei, L., Zádori, D., 2019. HPLC method for the assessment of tryptophan metabolism utilizing separate internal standard for each detector. *Anal. Biochem.* 574, 7–14.
<https://doi.org/10.1016/J.AB.2019.03.005>
- DeLapp, N.W., Gough, W.H., Kahl, S.D., Porter, A.C., Wiernicki, T.R., 2004. GTPγS Binding Assays, Assay Guidance Manual. Eli Lilly & Company and the National Center for Advancing Translational Sciences.
- Demuth, D.G., Molleman, A., 2006. Cannabinoid signalling. *Life Sci.* 78, 549–563.
<https://doi.org/10.1016/j.lfs.2005.05.055>
- Desfossés, J., Stip, E., Bentaleb, L.A., Potvin, S., 2010. Endocannabinoids and Schizophrenia. *Pharmaceuticals* 3, 3101–3126. <https://doi.org/10.3390/ph3103101>
- Dvorácskó, S., Keresztes, A., Mollica, A., Stefanucci, A., Macedonio, G., Pieretti, S., Zádor, F.,

- Walter, F.R., Deli, M.A., Kékesi, G., Bánki, L., Tuboly, G., Horváth, G., Tömböly, C., 2019. Preparation of bivalent agonists for targeting the mu opioid and cannabinoid receptors. *Eur. J. Med. Chem.* 178, 571–588. <https://doi.org/10.1016/j.ejmech.2019.05.037>
- Erhardt, S., Schwieler, L., Imbeault, S., Engberg, G., 2017. The kynurenine pathway in schizophrenia and bipolar disorder. *Neuropharmacology* 112, 297–306. <https://doi.org/10.1016/J.NEUROPHARM.2016.05.020>
- Fernández-Fernández, C., Callado, L.F., Girón, R., Sánchez, E., Erdozain, A.M., López-Moreno, J.A., Morales, P., Rodríguez de Fonseca, F., Fernández-Ruiz, J., Goya, P., Meana, J.J., Martín, M.I., Jagerovic, N., 2014. Combining rimonabant and fentanyl in a single entity: preparation and pharmacological results. *Drug Des. Devel. Ther.* 8, 263–277. <https://doi.org/10.2147/DDDT.S55045>
- Fernández-Ruiz, J., Hernández, M., Ramos, J.A., 2010. Cannabinoid-dopamine interaction in the pathophysiology and treatment of CNS disorders. *CNS Neurosci. Ther.* 16, e72-91. <https://doi.org/10.1111/j.1755-5949.2010.00144.x>
- Frey, K.A., Albin, R.L., 2001. Receptor binding techniques. *Curr. Protoc. Neurosci.* Chapter 1, Unit1.4. <https://doi.org/10.1002/0471142301.ns0104s00>
- Fukui, S., Schwarcz, R., Rapoport, S.I., Takada, Y., Smith, Q.R., 1991. Blood-brain barrier transport of kynurenines: implications for brain synthesis and metabolism. *J. Neurochem.* 56, 2007–17.
- Gérard, N., Pieters, G., Goffin, K., Bormans, G., Van Laere, K., 2011. Brain Type 1 Cannabinoid Receptor Availability in Patients with Anorexia and Bulimia Nervosa. *Biol. Psychiatry* 70, 777–784. <https://doi.org/10.1016/J.BIOPSYCH.2011.05.010>
- Gill, R., Woodruff, G.N., 1990. The neuroprotective actions of kynurenic acid and MK-801 in gerbils are synergistic and not related to hypothermia. *Eur. J. Pharmacol.* 176, 143–149. [https://doi.org/10.1016/0014-2999\(90\)90522-8](https://doi.org/10.1016/0014-2999(90)90522-8)
- Guo, J., Williams, D.J., Puhl, H.L., Ikeda, S.R., 2007. Inhibition of N-Type Calcium Channels by Activation of GPR35, an Orphan Receptor, Heterologously Expressed in Rat Sympathetic Neurons. *J. Pharmacol. Exp. Ther.* 324, 342–351. <https://doi.org/10.1124/jpet.107.127266>
- Herkenham, M., Lynn, A.B., Little, M.D., Johnson, M.R., Melvin, L.S., de Costa, B.R., Rice,

- K.C., 1990. Cannabinoid receptor localization in brain. *Proc. Natl. Acad. Sci. U. S. A.* 87, 1932–6.
- Howlett, a C., Barth, F., Bonner, T.I., Cabral, G., Casellas, P., Devane, W. a, Felder, C.C., Herkenham, M., Mackie, K., Martin, B.R., Mechoulam, R., Pertwee, R.G., 2002. International Union of Pharmacology. XXVII. Classification of cannabinoid receptors. *Pharmacol. Rev.* 54, 161–202.
- Ibarra-Lecue, I., Pilar-Cuéllar, F., Muguruza, C., Florensa-Zanuy, E., Díaz, Á., Urigüen, L., Castro, E., Pazos, A., Callado, L.F., 2018. The endocannabinoid system in mental disorders: Evidence from human brain studies. *Biochem. Pharmacol.* 157, 97–107.
<https://doi.org/10.1016/J.BCP.2018.07.009>
- Javitt, D.C., Schoepp, D., Kalivas, P.W., Volkow, N.D., Zarate, C., Merchant, K., Bear, M.F., Umbrecht, D., Hajos, M., Potter, W.Z., Lee, C.-M., 2011. Translating glutamate: from pathophysiology to treatment. *Sci. Transl. Med.* 3, 102mr2.
<https://doi.org/10.1126/scitranslmed.3002804>
- Jenny, M., Santer, E., Pirich, E., Schennach, H., Fuchs, D., 2009. Δ^9 -Tetrahydrocannabinol and cannabidiol modulate mitogen-induced tryptophan degradation and neopterin formation in peripheral blood mononuclear cells in vitro. *J. Neuroimmunol.* 207, 75–82.
<https://doi.org/10.1016/j.jneuroim.2008.12.004>
- Kenakin, T., 2001. Inverse, protean, and ligand-selective agonism: matters of receptor conformation. *FASEB J.* 15, 598–11.
- Knyihar-Csillik, E., Mihaly, A., Krisztin-Peva, B., Robotka, H., Szatmari, I., Fulop, F., Toldi, J., Csillik, B., Vecsei, L., 2008. The kynurenate analog SZR-72 prevents the nitroglycerol-induced increase of c-fos immunoreactivity in the rat caudal trigeminal nucleus: comparative studies of the effects of SZR-72 and kynurenic acid. *Neurosci. Res.* 61, 429–32.
<https://doi.org/10.1016/j.neures.2008.04.009>
- Krishna Kumar, K., Shalev-Benami, M., Robertson, M.J., Hu, H., Banister, S.D., Hollingsworth, S.A., Latorraca, N.R., Kato, H.E., Hilger, D., Maeda, S., Weis, W.I., Farrens, D.L., Dror, R.O., Malhotra, S. V., Kobilka, B.K., Skinotis, G., 2019. Structure of a Signaling Cannabinoid Receptor 1-G Protein Complex. *Cell* 176, 448–458.e12.

<https://doi.org/10.1016/J.CELL.2018.11.040>

- Le Naour, M., Akgün, E., Yekkirala, A., Lunzer, M.M., Powers, M.D., Kalyuzhny, A.E., Portoghese, P.S., 2013. Bivalent ligands that target μ opioid (MOP) and cannabinoid1 (CB1) receptors are potent analgesics devoid of tolerance. *J. Med. Chem.* 56, 5505–5513. <https://doi.org/10.1021/jm4005219>
- Lee, D.Y., Lee, K.-S., Lee, H.J., Noh, Y.H., Kim, D.H., Lee, J.Y., Cho, S.H., Yoon, O.J., Lee, W.B., Kim, K.Y., Chung, Y.H., Kim, S.S., 2008. Kynurenic acid attenuates MPP(+)-induced dopaminergic neuronal cell death via a Bax-mediated mitochondrial pathway. *Eur. J. Cell Biol.* 87, 389–97. <https://doi.org/10.1016/j.ejcb.2008.03.003>
- Maccarrone, M., Bab, I., Bíró, T., Cabral, G.A., Dey, S.K., Di Marzo, V., Konje, J.C., Kunos, G., Mechoulam, R., Pacher, P., Sharkey, K.A., Zimmer, A., 2015. Endocannabinoid signaling at the periphery: 50 years after THC. *Trends Pharmacol. Sci.* <https://doi.org/10.1016/j.tips.2015.02.008>
- Mackie, K., 2005. Distribution of cannabinoid receptors in the central and peripheral nervous system. *Handb. Exp. Pharmacol.* 299–325.
- Mándi, Y., Vécsei, L., 2012. The kynurenine system and immunoregulation. *J. Neural Transm.* 119, 197–209. <https://doi.org/10.1007/s00702-011-0681-y>
- Matsuda, L.A., Lolait, S.J., Brownstein, M.J., Young, A.C., Bonner, T.I., 1990. Structure of a cannabinoid receptor and functional expression of the cloned cDNA. *Nature* 346, 561–564. <https://doi.org/10.1038/346561a0>
- Miller, L.K., Devi, L.A., 2011. The Highs and Lows of Cannabinoid Receptor Expression in Disease: Mechanisms and Their Therapeutic Implications. *Pharmacol. Rev.* 63, 461–470. <https://doi.org/10.1124/pr.110.003491>
- Milligan, G., 2011. Orthologue selectivity and ligand bias: translating the pharmacology of GPR35. *Trends Pharmacol. Sci.* 32, 317–325. <https://doi.org/10.1016/j.tips.2011.02.002>
- Mollica, A., Pelliccia, S., Famiglini, V., Stefanucci, A., Macedonio, G., Chiavaroli, A., Orlando, G., Brunetti, L., Ferrante, C., Pieretti, S., Novellino, E., Benyhe, S., Zador, F., Erdei, A., Szucs, E., Samavati, R., Dvrorasko, S., Tomboly, C., Ragno, R., Patsilnakos, A., Silvestri, R., 2017. Exploring the first Rimonabant analog-opioid peptide hybrid compound, as

- bivalent ligand for CB1 and opioid receptors. *J. Enzyme Inhib. Med. Chem.* 32, 444–451. <https://doi.org/10.1080/14756366.2016.1260565>
- Nagy-Grócz, G., Zádor, F., Dvorácskó, S., Bohár, Z., Benyhe, S., Tömböly, C., Párdutz, Á., Vécsei, L., 2017. Interactions between the Kynurenine and the Endocannabinoid System with Special Emphasis on Migraine. *Int. J. Mol. Sci.* 18, 1617. <https://doi.org/10.3390/ijms18081617>
- Neumeister, A., Seidel, J., Ragen, B.J., Pietrzak, R.H., 2015. Translational evidence for a role of endocannabinoids in the etiology and treatment of posttraumatic stress disorder. *Psychoneuroendocrinology* 51, 577–84. <https://doi.org/10.1016/j.psycheneu.2014.10.012>
- Nilsson, L.K., Linderholm, K.R., Erhardt, S., 2006. Subchronic treatment with kynurenine and probenecid: effects on prepulse inhibition and firing of midbrain dopamine neurons. *J. Neural Transm.* 113, 557–571. <https://doi.org/10.1007/s00702-005-0343-z>
- Ohshiro, H., Tonai-Kachi, H., Ichikawa, K., 2008. GPR35 is a functional receptor in rat dorsal root ganglion neurons. *Biochem. Biophys. Res. Commun.* 365, 344–348. <https://doi.org/10.1016/j.bbrc.2007.10.197>
- Oláh, G., Herédi, J., Menyhárt, A., Czinege, Z., Nagy, D., Fuzik, J., Kocsis, K., Knapp, L., Krucsó, E., Gellért, L., Kis, Z., Farkas, T., Fülöp, F., Párdutz, A., Tajti, J., Vécsei, L., Toldi, J., 2013. Unexpected effects of peripherally administered kynurenic acid on cortical spreading depression and related blood-brain barrier permeability. *Drug Des. Devel. Ther.* 7, 981–7. <https://doi.org/10.2147/DDDT.S44496>
- Pacher, P., Bátkai, S., Kunos, G., 2006. The endocannabinoid system as an emerging target of pharmacotherapy. *Pharmacol. Rev.* 58, 389–462. <https://doi.org/10.1124/pr.58.3.2>
- Pagotto, U., Marsicano, G., Cota, D., Lutz, B., Pasquali, R., 2006. The Emerging Role of the Endocannabinoid System in Endocrine Regulation and Energy Balance. *Endocr. Rev.* 27, 73–100. <https://doi.org/10.1210/er.2005-0009>
- Párdutz, A., Fejes, A., Bohár, Z., Tar, L., Toldi, J., Vécsei, L., 2012. Kynurenines and headache. *J. Neural. Transm.* 119, 285–96. <https://doi.org/10.1007/s00702-011-0665-y>
- Perkins, M.N., Stone, T.W., 1985. Actions of kynurenic acid and quinolinic acid in the rat hippocampus in vivo. *Exp. Neurol.* 88, 570–9.

- Pertwee, R.G., 2009. Cannabinoid pharmacology: the first 66 years. *Br. J. Pharmacol.* 147, S163–S171. <https://doi.org/10.1038/sj.bjp.0706406>
- Piomelli, D., 2003. The molecular logic of endocannabinoid signalling. *Nat. Rev. Neurosci.* 4, 873–884. <https://doi.org/10.1038/nrn1247>
- R Core Team, 2014. R: A Language and Environment for Statistical Computing. R Foundation for Statistical Computing, Vienna, Austria.
- Rodríguez de Fonseca, F., Del Arco, I., Bermudez-Silva, F.J., Bilbao, A., Cippitelli, A., Navarro, M., 2005. The endocannabinoid system: physiology and pharmacology. *Alcohol Alcohol* 40, 2–14. <https://doi.org/10.1093/alcalc/agh110>
- Samavati, R., Zádor, F., Szűcs, E., Tuka, B., Martos, D., Veres, G., Gáspár, R., Mándity, I.M., Fülöp, F., Vécsei, L., Benyhe, S., Borsodi, A., 2017. Kynurenic acid and its analogue can alter the opioid receptor G-protein signaling after acute treatment via NMDA receptor in rat cortex and striatum. *J. Neurol. Sci.* 376, 63–70. <https://doi.org/10.1016/j.jns.2017.02.053>
- Scharfman, H., Goodman, J., 1998. Effects of central and peripheral administration of kynurenic acid on hippocampal evoked responses in vivo and in vitro. *Neuroscience* 86, 751–764. [https://doi.org/10.1016/S0306-4522\(98\)00073-6](https://doi.org/10.1016/S0306-4522(98)00073-6)
- Secci, M.E., Mascia, P., Sagheddu, C., Beggiano, S., Melis, M., Borelli, A.C., Tomasini, M.C., Panlilio, L. V., Schindler, C.W., Tanda, G., Ferré, S., Bradberry, C.W., Ferraro, L., Pistis, M., Goldberg, S.R., Schwarcz, R., Justinova, Z., 2018. Astrocytic Mechanisms Involving Kynurenic Acid Control Δ^9 -Tetrahydrocannabinol-Induced Increases in Glutamate Release in Brain Reward-Processing Areas. *Mol. Neurobiol.* 1–13. <https://doi.org/10.1007/s12035-018-1319-y>
- Selley, D.E., Sim, L.J., Xiao, R., Liu, Q., Childers, S.R., 1997. μ -Opioid receptor-stimulated guanosine-5'-O-(gamma-thio)-triphosphate binding in rat thalamus and cultured cell lines: signal transduction mechanisms underlying agonist efficacy. *Mol. Pharmacol.* 51, 87–96.
- Shore, D.M., Reggio, P.H., 2015. The therapeutic potential of orphan GPCRs, GPR35 and GPR55. *Front. Pharmacol.* 6, 69. <https://doi.org/10.3389/fphar.2015.00069>
- Silva-Adaya, D., Pérez-De La Cruz, V., Villeda-Hernández, J., Carrillo-Mora, P., González-Herrera, I.G., García, E., Colín-Barenque, L., Pedraza-Chaverrí, J., Santamaría, A., 2011.

- Protective effect of l-kynurenine and probenecid on 6-hydroxydopamine-induced striatal toxicity in rats: Implications of modulating kynurenate as a protective strategy. *Neurotoxicol. Teratol.* 33, 303–312. <https://doi.org/10.1016/J.NTT.2010.10.002>
- Stone, J.M., Morrison, P.D., Pilowsky, L.S., 2007. Review: Glutamate and dopamine dysregulation in schizophrenia — a synthesis and selective review. *J. Psychopharmacol.* 21, 440–452. <https://doi.org/10.1177/0269881106073126>
- Strange, P.G., 2010. Use of the GTP γ S ([³⁵S]GTP γ S and Eu-GTP γ S) binding assay for analysis of ligand potency and efficacy at G protein-coupled receptors. *Br. J. Pharmacol.* 161, 1238–49. <https://doi.org/10.1111/j.1476-5381.2010.00963.x>
- Szalardy, L., Zadori, D., Toldi, J., Fulop, F., Klivenyi, P., Vecsei, L., 2012. Manipulating kynurenic acid levels in the brain - on the edge between neuroprotection and cognitive dysfunction. *Curr. Top. Med. Chem.* 12, 1797–806.
- Szücs, E., Dvorácskó, S., Tömböly, C., Büki, A., Kékesi, G., Horváth, G., Benyhe, S., 2016. Decreased CB receptor binding and cannabinoid signaling in three brain regions of a rat model of schizophrenia. *Neurosci. Lett.* 633, 87–93. <https://doi.org/10.1016/J.NEULET.2016.09.020>
- Szücs, E., Stefanucci, A., Dimmito, M.P., Zádor, F., Pieretti, S., Zengin, G., Vécsei, L., Benyhe, S., Nalli, M., Mollica, A., 2020. Discovery of Kynurenines Containing Oligopeptides as Potent Opioid Receptor Agonists. *Biomolecules* 10, 284. <https://doi.org/10.3390/biom10020284>
- Taniguchi, Y., Tonai-Kachi, H., Shinjo, K., 2006. Zaprinast, a well-known cyclic guanosine monophosphate-specific phosphodiesterase inhibitor, is an agonist for GPR35. *FEBS Lett.* 580, 5003–5008. <https://doi.org/10.1016/j.febslet.2006.08.015>
- Traynor, J., Nahorski, S., 1995. Modulation by mu-opioid agonists of guanosine-5'-O-(3-[³⁵S]thio)triphosphate binding to membranes from human neuroblastoma SH-SY5Y cells. *Mol. Pharmacol.* 47, 848–854.
- Varga, D., Herédi, J., Kánvási, Z., Ruszka, M., Kis, Z., Ono, E., Iwamori, N., Iwamori, T., Takakuwa, H., Vécsei, L., Toldi, J., Gellért, L., 2015. Systemic L-Kynurenine sulfate administration disrupts object recognition memory, alters open field behavior and decreases

- c-Fos immunopositivity in C57Bl/6 mice. *Front. Behav. Neurosci.* 9, 157.
<https://doi.org/10.3389/fnbeh.2015.00157>
- Vécsei, L., Szalárdy, L., Fülöp, F., Toldi, J., 2013. Kynurenines in the CNS: recent advances and new questions. *Nat. Rev. Drug. Discov.* 12, 64–82. <https://doi.org/10.1038/nrd3793>
- Venkatakrishnan, a J., Deupi, X., Lebon, G., Tate, C.G., Schertler, G.F., Babu, M.M., 2013. Molecular signatures of G-protein-coupled receptors. *Nature* 494, 185–94.
<https://doi.org/10.1038/nature11896>
- Viganò, D., Rubino, T., Parolaro, D., 2005. Molecular and cellular basis of cannabinoid and opioid interactions. *Pharmacol. Biochem. Behav.* 81, 360–368.
<https://doi.org/10.1016/j.pbb.2005.01.021>
- Wang, J., Simonavicius, N., Wu, X., Swaminath, G., Reagan, J., Tian, H., Ling, L., 2006. Kynurenic Acid as a Ligand for Orphan G Protein-coupled Receptor GPR35. *J. Biol. Chem.* 281, 22021–22028. <https://doi.org/10.1074/JBC.M603503200>
- Wu, H.-Q., Guidetti, P., Goodman, J., Varasi, M., Ceresoli-Borroni, G., Speciale, C., Scharfman, H., Schwarcz, R., 2000. Kynurenergic manipulations influence excitatory synaptic function and excitotoxic vulnerability in the rat hippocampus in vivo. *Neuroscience* 97, 243–251.
[https://doi.org/10.1016/S0306-4522\(00\)00030-0](https://doi.org/10.1016/S0306-4522(00)00030-0)
- Zádor, F., Kocsis, D., Borsodi, A., Benyhe, S., 2014a. Micromolar concentrations of rimonabant directly inhibits delta opioid receptor specific ligand binding and agonist-induced G-protein activity. *Neurochem. Int.* 67, 14–22. <https://doi.org/10.1016/j.neuint.2013.12.005>
- Zádor, F., Nagy-Grócz, G., Kekesi, G., Dvorácskó, S., Szűcs, E., Tömböly, C., Horvath, G., Benyhe, S., Vécsei, L., 2019. Kynurenines and the Endocannabinoid System in Schizophrenia: Common Points and Potential Interactions. *Molecules* 24, 3709.
<https://doi.org/10.3390/molecules24203709>
- Zádor, F., Samavati, R., Szlávicz, E., Tuka, B., Bojnik, E., Fülöp, F., Toldi, J., Vécsei, L., Borsodi, A., 2014b. Inhibition of Opioid Receptor Mediated G-Protein Activity After Chronic Administration of Kynurenic Acid and its Derivative without Direct Binding to Opioid Receptors. *CNS Neurol. Disord. - Drug Targets* 13, 1520–1529.
- Zádori, D., Klivényi, P., Plangár, I., Toldi, J., Vécsei, L., 2011a. Endogenous neuroprotection in

chronic neurodegenerative disorders: with particular regard to the kynurenines. *J Cell Mol Med* 15, 701–17. <https://doi.org/10.1111/j.1582-4934.2010.01237.x>

Zádori, D., Nyiri, G., Szonyi, A., Szatmári, I., Fülöp, F., Toldi, J., Freund, T.F., Vécsei, L., Klivényi, P., 2011b. Neuroprotective effects of a novel kynurenic acid analogue in a transgenic mouse model of Huntington's disease. *J Neural Transm* 118, 865–75. <https://doi.org/10.1007/s00702-010-0573-6>

Zhao, P., Lane, T.R., Gao, H.G.L., Hurst, D.P., Kotsikorou, E., Le, L., Brailoiu, E., Reggio, P.H., Abood, M.E., 2014. Crucial positively charged residues for ligand activation of the GPR35 receptor. *J. Biol. Chem.* 289, 3625–38. <https://doi.org/10.1074/jbc.M113.508382>